Adult-onset nicotinamide supplementation prevents the emergence of early-life stress driven inflammatory signatures, blood-brain barrier compromise, hippocampal mitochondrial dysfunction and cognitive aging

Pratik Chaudhari

pratikchaudhari11@gmail.com

Tata Institute of Fundamental Research https://orcid.org/0000-0001-6873-0446

Nishtha Pange

Tata Institute of Fundamental Research

Aastha Singla

Tata Institute of Fundamental Research

Shital Suryavanshi

Tata Institute of Fundamental Research

Kowshik Kukkemane

Tata Institute of Fundamental Research

Pradip Chaudhari

Advanced Centre for Treatment, Research & Education in Cancer, Tata Memorial Centre

Bhabani Shankar Mohanty

Advanced Centre for Treatment, Research & Education in Cancer, Tata Memorial Centre

Ratna Mahathi Vuruputuri

Tata Institute of Fundamental Research

Anshit Singh

Tata Institute of Fundamental Research

Sashaina Fanibunda

Kasturba Integrative Health Sciences- Medical Research Foundation

Shalaka Masurkar

Department of Biosciences and Bioengineering, Indian Institute of Technology Bombay

Deepika Suri

Tata Institute of Fundamental Research

Praachi Tiwari

Tata Institute of Fundamental Research

Amartya Pradhan
Tata Institute of Fundamental Research
Darshana Kapri
Tata Institute of Fundamental Research
Suchith Mendon
Tata Institute of Fundamental Research
Biju Viswanath
Department of Psychiatry, National Institute of Mental Health and Neurosciences
Samir Maji
Department of Biosciences and Bioengineering, Indian Institute of Technology Bombay
Ullas Kolthur-Seetharam
Tata Institute of Fundamental Research
Ashok Vaidya
Kasturba Integrative Health Sciences- Medical Research Foundation
Carmen Sandi
Brain Mind Institute, Ecole Polytechnique Federale de Lausanne
Vidita Vaidya
Tata Institute of Fundamental Research

Article

Keywords:

Posted Date: February 25th, 2026

DOI: https://doi.org/10.21203/rs.3.rs-8934974/v1

Additional Declarations: There is **NO** Competing Interest.

Adult-onset nicotinamide supplementation prevents the emergence of early-life stress driven inflammatory signatures, blood-brain barrier compromise, hippocampal mitochondrial dysfunction and cognitive aging

Authors

Pratik R. Chaudhari[1*], Nishtha Pange[1], Aastha Singla[1], Shital Suryavanshi[1], Kowshik Kukkemane[1], Pradip Chaudhari[2,3], Bhabani Shankar Mohanty[2], Ratna Mahathi Vuruputuri[1], Anshit Singh[1], Sashaina E. Fanibunda[1,4], Shalaka A. Masurkar[5,6], Deepika Suri[1], Praachi Tiwari[1], Amartya Pradhan[1], Darshana Kapri[1], Suchith Mendon[1], Biju Viswanath[7], Samir K. Maji[5,6], Ullas Kolthur-Seetharam[1], Ashok D. B. Vaidya[4], Carmen Sandi[8], Vidita A. Vaidya[1*]

Affiliations

[1]Department of Biological Sciences, Tata Institute of Fundamental Research, Mumbai, India
[2]Advanced Centre for Treatment, Research & Education in Cancer, Tata Memorial Centre, Navi Mumbai, India
[3]Homi Bhabha National Institute, BARC Training School Complex, Mumbai, India
[4]Kasturba Integrative Health Sciences- Medical Research Foundation, Mumbai, India
[5]Department of Biosciences and Bioengineering, Indian Institute of Technology Bombay, Mumbai, India
[6]Sunita Sanghi Centre of Aging and Neurodegenerative Diseases, Indian Institute of Technology Bombay, Mumbai, India
[7]Department of Psychiatry, National Institute of Mental Health and Neurosciences, Bengaluru, Karnataka, India
[8]Brain Mind Institute, Ecole Polytechnique Federale de Lausanne, Lausanne, Switzerland

Corresponding authorship

* Equal corresponding authors

Author contributions

Conceptualization: P.R.C., A.D.B.V., C.S., V.A.V.
Funding acquisition: P.R.C., V.A.V.
Investigation and data analysis: P.R.C., N.P., A.S., S.S., K.K., P.C., B.S.M., R.M.V., A.S.2, S.E.F., S.A.M., D.S., P.T., A.P., D.K., V.A.V.
Data interpretation: P.R.C., V.A.V.
Supervision: P.R.C., U.K.S., A.D.B.V., C.S., V.A.V.
Resources: B.V., S.K.M., U.K.S.
Writing: P.R.C., C. S., V.A.V.

Abstract

Growing evidence suggests that early-life stress history can shape biological aging, yet the pathways through which this lifelong vulnerability manifests remain unclear. Using a maternal separation (MS) rodent model of early-life stress, we show that MS history evokes persistent cognitive, inflammatory, neurovasculature and bioenergetic changes that can accelerate aging trajectories. MS animals exhibit premature decline in object recognition memory in middle-aged life, accompanied by elevated peripheral inflammation, blood-brain barrier (BBB) compromise, heightened neuroinflammasome and microglial reactivity, and deteriorated mitochondrial health in the hippocampus. Notably, we demonstrate that adult-onset systemic supplementation with Nicotinamide (NAM), a NAD^+ precursor, prevents the emergence of peripheral and central inflammatory signatures, protects BBB integrity, maintains hippocampal mitochondrial health and mitigates cognitive decline in middle-aged MS animals. Collectively, these findings provide mechanistic insights into how early-life stress shapes brain aging, while highlighting NAM supplementation as a gerotherapeutic strategy to prevent premature aging driven by early adversity.

Main

Early adversity, in addition to heightening vulnerability for the development of adult psychopathology, can also enhance risk for cognitive dysfunction and evoke signatures of premature aging [1–5]. Several of the immune, metabolic, cellular and cognitive sequelae of early-life stress overlap with hallmark signatures of aging [6–8]. Studies in rodent models of early-life stress, focussed on disruption of dam-pup interactions, evoke a broad range of physiological and neurological sequelae [5,8–11]. These early-life stress models, including the most prevalent model of maternal separation (MS) [12], perturb neuroendocrine stress responses, disrupt anxio-depressive, social and reward-related behaviours in adulthood, enhance inflammation, impair hippocampal plasticity and hasten cognitive decline in middle-aged life, underscoring the relatively persistent nature of maladaptive responses [13–19]. Given the time and logistical constraints of life-course analyses, most early-life stress studies have predominantly focussed on time windows spanning up to young adulthood with a few studies performed in aging animals [8,9,11,17,20–24], limiting our understanding of the sequelae that emerge progressively later in life.

We hypothesized that perturbed mitochondrial homeostasis and neurovascular compromise, are relevant MS-induced alterations, accompanied by elevated peripheral and central inflammatory markers and altered cognitive performance, emerging progressively across the temporal epochs of mature adulthood (6-7 months) and middle-age (13-15 months). We focused on the hippocampus given the high vulnerability of this major limbic brain region to stress, and its top-down role in the modulation of stress responses [25,26]. We posited that these changes were likely to emerge slowly, providing for a temporal window in which to directly test whether putative gerotherapeutics like the nicotinamide adenine dinucleotide (NAD^+) precursor [27], nicotinamide (NAM), could mitigate the hastening of aging-related signatures in MS animals. NAM, in addition to restoring aging-associated depletion of tissue NAD^+ levels, is thought to target mitochondrial function, protect neurovasculature, and dampen inflammation in late life [27–30]; however, whether it can counteract early-life stress accelerated aging trajectories has not been tested. We find that MS produces distinct temporal trajectories for peripheral and central inflammatory signatures, with the gradual emergence of inflammation initially noted in the periphery in mature adulthood, that progressively worsens with strong neuroinflammatory changes in the hippocampus in middle-aged life. MS also evokes compromised blood-brain barrier (BBB) integrity, deterioration of hippocampal mitochondrial health and cognitive decline noted in middle-aged life. We find that systemic long-term NAM supplementation, commencing in mature adulthood, can prevent the impact of MS on peripheral and central inflammatory signatures, neurovascular compromise, hippocampal mitochondrial status and cognitive performance in middle-aged life, providing mechanistic insights into how early-life stress shapes brain aging and how a NAD^+ boosting intervention can intercept these trajectories.

Results

Early-life stress impairs object recognition memory and enhances peripheral inflammation in middle-aged rats

We sought to address the long-term consequences of MS in Sprague-Dawley (SD) rats at temporal epochs of mature adulthood (6-7 months) and in middle-aged life (13-15 months), commencing with assessing object recognition memory using the Novel Object Recognition (NOR) task (Fig. 1a-c, Extended data 1a-c). Middle-aged MS animals of both sexes exhibited reduced short and long-term object recognition memory (Fig. 1c, Extended data 2), with no such cognitive decline noted in mature adulthood (Extended data 1c). The discrimination index of middle-aged MS animals was significantly reduced compared to age-matched control cohorts, and was comparable to that of aged (22 month) controls (Extended data 3), suggesting accelerated cognitive decline.

We next evaluated peripheral markers of aging and inflammation in the control and MS middle-aged male and female cohort assessed for cognitive behaviour (Fig. 1d). Middle-aged MS rats, independent of sex, exhibited significant increases in circulating growth derived factor 15 (GDF15), a stress-responsive biomarker for aging, and in pro-inflammatory markers like C-reactive protein (CRP), interleukin1ß (IL1ß), interferon-γ (IFNγ), and tumour necrosis factor-α (TNFα) levels (Fig. 1e-i) and a decline in the anti-inflammatory cytokine, IL10 (Fig. 1j). Cross-correlational analyses of these serum markers with NOR scores revealed a significant inverse correlation between cognitive performance and GDF15, CRP, IL1ß, IFNγ, TNFα levels in middle-aged MS rats, with a positive correlation noted for IL10 (Extended data 4c). No significant correlations between cognitive performance and these peripheral markers was observed in the age-matched controls (Extended data 4d). These findings indicate that a history of MS is associated with enhanced peripheral inflammation in middle-aged life that corresponds to a deteriorated cognitive performance.

Given limited serum availability for profiling additional markers, we used an independent cohort of middle-aged control and MS rats not subjected to behavioural analyses, to examine IL4, IL6, IL18, methylglyoxal, and kynurenine (Fig. 1k-p). We noted a significant reduction in the anti-inflammatory cytokine IL4 and increases in IL6 and IL18 levels in middle-aged MS rats (Fig. 1l-n). Furthermore, middle-aged MS animals exhibited elevated levels of the precursor for advanced glycation end-products (AGEs), methylglyoxal, and the inflammaging-associated, tryptophan catabolism intermediate, kynurenine (Fig. 1o-p). We next assessed stress and aging-associated markers, including circulating cell free mitochondrial DNA (ccf-mtDNA), and corticosterone, and noted significant increases in middle-aged MS animals (Fig. 1q-r). Complete blood count analysis revealed inflammatory signatures of increased total white blood cells (WBCs) and platelet counts in middle-aged MS male rats (Extended data 5c).

We then asked whether enhanced expression of inflammation and aging-associated peripheral markers was already evident in MS animals in mature adulthood, a time-point at which cognitive decline had not yet set in. MS rats of both sexes in mature adulthood displayed small, but significant, increases in GDF15, CRP, IL1ß, IL18 and ccf-mtDNA content (Extended data 1e-g, m-n), with no change in IFNγ, TNFα, IL10, IL4, and IL6 levels (Extended data 1h-l). We did not observe alterations in the complete blood count profile in MS male rats in mature adulthood (Extended data 5b). Taken together, we find that MS history progressively enhances peripheral pro-inflammatory markers, including several cytokines and CRP, disrupts metabolic signatures associated with aging, namely GDF15, methylglyoxal, kynurenine, and elevates

stress-associated peripheral signatures, such as corticosterone, ccf-mtDNA and haematological changes in middle-aged life. Specific aspects of these systemic signatures are already apparent in mature adulthood, albeit with reduced severity that appears to cumulatively worsen into middle-aged life.

Early-life stress disrupts the blood-brain barrier integrity in middle-aged animals

Since systemic inflammation is closely associated with neurovascular dysfunction[31] and stress has been linked to alterations in BBB function [32,33], we next explored the influence of MS on the BBB (Fig. 2a). We evaluated the hippocampal expression of genes associated with BBB formation and maintenance, tight junctions, and neurovasculature in middle-aged life and observed significant decreases in netrin1 (*Ntn1*), major facilitator superfamily domain-containing protein-2a (*Mfsd2a*), claudin5 (*Cld5*), claudin1 (*Cld1*), occludin (*Ocln*), tight junction protein ZO-3 (*Tjp3*), melanoma cell adhesion molecule (*Cd146*), and aquaporin4 (*Aqp4*) in the hippocampi of middle-aged MS animals (Fig. 2c), which was not observed in mature adulthood (Fig. 2b). Next, we assessed BBB integrity using both biochemical (Fig. 2d-f) and radioimaging assays (Fig. 2g-i). The Evans blue extravasation assay indicated a compromised BBB in the hippocampal parenchyma of middle-aged MS animals (Fig. 2f), with no such BBB leakiness noted in mature adulthood (Fig. 2e). Further, *ex-vivo* SPECT (Single Photon Emission Computed Tomography) scans revealed presence of the radiotracer Technitium-99 (99mTc) in the brain parenchyma of middle-aged MS male rats (Fig. 2i), while no neurovascular leak was noted in mature adulthood (Fig. 2h). We then assessed soluble E-selectin (sE-selectin), a serum marker of endothelial activation and systemic inflammation that contributes to BBB disruption [34], and noted robust upregulation in sE-selectin levels in middle-aged MS animals (Fig. 2l), an effect absent in mature adulthood (Fig. 2k). We next assessed hippocampal IFN-γ levels given prior evidence that IFN-γ impacts BBB function increasing permeability [35], and noted significantly higher IFNγ levels in the hippocampi of middle-aged MS rats (Fig. 2m), with IFNγ undetectable in the hippocampus in mature adulthood. Our results reveal a concurrent rise in systemic sE-selectin and hippocampal IFN-γ levels suggestive of an inflammatory state and endothelial activation that accompanies BBB disruption in middle-aged MS animals.

Early-life stress enhances neuroinflammatory signatures and disrupts mitochondrial function in the hippocampus in middle-aged life

Given our findings of significant peripheral inflammation and BBB fragility in middle-aged MS animals, we next assessed neuroinflammation in the hippocampi of MS male rats, in both mature adulthood and middle-aged life. We examined expression of components of the NLRP3 inflammasome (NOD-, LRR- and pyrin domain-containing protein 3: NLRP3, Apoptosis-associated speck-like protein containing a CARD: ASC), and of NFκB, a key regulator of NLRP3 inflammasome priming, and noted robust increases in NLRP3, ASC, and NFκB hippocampal protein levels in middle-aged MS animals (Fig. 3b-c). We then assessed cellular markers of neuroinflammation within the hippocampus by examining microglial activation using IBA1 immunostaining (Fig. 3d) and noted significantly increased numbers of activated microglia in all hippocampal subfields of middle-aged MS animals (Fig. 3e-h). MS animals in

mature adulthood did not show changes in either inflammasome protein levels or in activated microglial numbers in the hippocampus (Extended data 6b-c, d-g).

Taking into account the reciprocal relationship between mitochondria and inflammation [36], and that stress is a strong modulator of mitochondrial functions [37,38], we hypothesized that the robust neuroinflammatory changes in the hippocampi of middle-aged MS animals would be accompanied by evidence of perturbed mitochondrial status. We noted significant decreases in hippocampal mtDNA content in middle-aged MS rats of both sexes (Fig. 3i), accompanied by a reduction in cellular ATP levels (Fig. 3j). Further, we observed reduced protein expression of key regulators of mitochondrial biogenesis and function, peroxisome proliferator-activated receptor gamma coactivator 1α (PGC-1α), sirtuin 1 (SIRT1), and mitochondrial transcription factor A (TFAM) in the hippocampi of middle-aged MS male rats (Fig. 3k-l), in line with alterations in these molecules reported in the context of stress and aging [39–41]. Accompanying the changes in mitochondrial mass, we noted enhanced levels of mitochondrial reactive oxygen species (ROS) levels, measured via elevated levels of mitochondrial H_2O_2 (mtH_2O_2) in the hippocampi of middle-aged MS male rats (Fig. 3m). Analyses of mitochondrial respiration revealed striking alterations in the oxygen consumption rate (OCR), with a decline in state-2, state-3 and state-4 respiration in mitochondria derived from the hippocampi of middle-aged MS male rats (Fig. 3n-o). The reduction in mtDNA content and cellular ATP levels, as well as the increase in mitochondrial ROS production noted in the hippocampi of MS animals in middle-aged life was not observed in MS animals in mature adulthood (Extended data 7). Collectively, these results reveal that a MS history drives the gradual emergence of neuroinflammation and mitochondrial impairment in the hippocampus in middle-aged life, a time-point coincident with the breakdown of BBB integrity and cognitive decline.

Nicotinamide supplementation attenuates the impact of early-life stress on cognitive decline that emerges in middle-aged life

Considering the deleterious effects of MS are gradual in onset with limited consequences in mature adulthood, it provides a temporal window in which gerotherapeutics could be deployed to mitigate the impact of early-life stress. We examined the influence of a systemic intervention with nicotinamide (NAM), a precursor for NAD^+ biosynthesis. NAD^+ levels are known to decline with age and contribute to aging-associated inflammation and mitochondrial dysfunction [27]. We hypothesized that enhancing NAD^+ levels, via NAM supplementation commencing from mature adulthood, may protect against the impact of the early-life stress on premature aging. We treated control and MS cohorts with vehicle or NAM (100 mg/kg/day) supplementation in drinking water commencing at eight months of age for a duration of five months [Fig. 4a; Treatment groups: control and MS animals on regular drinking water (CD; MSD); control and MS animals on NAM supplemented drinking water (CN; MSN)]. Two-way ANOVA analyses revealed a significant MS×NAM interaction effect for hippocampal NAD^+ levels (Fig. 4b), with NAM supplementation preventing the hippocampal reduction in NAD^+ levels in middle-aged MS animals. NAM supplementation in control cohorts did not further boost hippocampal NAD^+ levels above that observed in vehicle-treated controls (Fig. 4b). We assessed the impact of NAM supplementation on cognitive performance (Fig. 4c), and noted a

significant MS×NAM interaction effect on two-way ANOVA analysis for both short and long-term object recognition memory (Fig. 4d-e). The significant decline observed in short and long-term discrimination indices in middle-aged MS male and female rats, was prevented by NAM supplementation (Fig. 4d-e). These results uncover a powerful effect of NAM supplementation in restoring hippocampal tissue levels of NAD^+ in middle-aged MS animals and in preventing cognitive decline.

Nicotinamide supplementation attenuates the impact of early-life stress on peripheral inflammation in middle-aged life

We then assessed the impact of NAM supplementation on serum markers of aging, inflammation, and stress in middle-aged MS and control male and female rats. Two-way ANOVA analyses revealed a significant MS×NAM interaction effect for GDF15, CRP, methylglyoxal, IFNγ, and IL1ß levels (Fig. 5b-f), with the significant increases noted in GDF15, CRP, and IFNγ in middle-aged MS rats prevented by NAM supplementation (Fig. 5b-c, e). Further, two-way ANOVA analyses indicated a significant MS×NAM interaction effect for ccf-mtDNA content and corticosterone, with the increases noted in MS animals in middle-aged life mitigated by NAM treatment (Fig. 5g-h). With regards to haematological profiling, we observed a significant MS×NAM interaction effect on two-way ANOVA, with the increased WBC and platelet counts in middle-aged MS male rats ameliorated in NAM supplemented MS cohort (Fig. 5i). While we noted a trend towards a significant MS×NAM ANOVA interaction for circulating levels of extracellular nicotinamide phosphoribosyl transferase (eNAMPT), a key adipokine involved in NAD^+ biosynthesis pathway, and the cytokines IL6 and IL10 (Extended data 8b-d), we did not observe any impact of NAM supplementation on circulating TNFα levels (Extended data 8e). Control cohorts supplemented with NAM did not exhibit any changes in these serum profiling and haematological analyses, suggesting that long-term NAM supplementation may not impact these inflammation-related measures in middle-aged controls. Our results reveal that NAM supplementation commencing in mature adulthood, when the first peripheral inflammatory signatures appear, can successfully avert the emergence of the long-term deleterious consequences of MS on peripheral inflammatory, stress and aging-associated markers.

Nicotinamide supplementation protects blood-brain barrier integrity in middle-aged MS rats

In light of our findings that NAM supplementation protects against systemic inflammation in middle-aged MS animals, we investigated the impact on safeguarding the BBB (Fig. 6a). Two-way ANOVA analyses revealed a significant MS×NAM interaction effect for radiotracer 99mTc counts in brain parenchyma evaluated using *ex-vivo* SPECT scans (Fig. 6b-c), with *post-hoc* analyses indicating that the increased BBB permeability noted in middle-aged MS animals was completely prevented by long-term NAM supplementation (Fig. 6c). We then examined whether NAM supplementation can prevent the MS-evoked dysregulation of hippocampal BBB-associated gene expression in middle-aged life (Fig. 6d). Two-way ANOVA analyses indicated a significant MS×NAM interaction effect for a subset of BBB-associated genes, *Ntn1*, *Mfsd2a, Ocln,* and *Aqp4,* with their decline in middle-aged MS animals prevented by NAM supplementation (Fig. 6d). We noted a significant MS×NAM two-way

ANOVA interaction for circulating sE-selectin and hippocampal IFNγ levels, with the increase in these measures observed in middle-aged MS animals averted by NAM supplementation (Fig. 6e-f). These results indicate that adult-onset NAM supplementation can preserve neurovasculature integrity in middle-aged MS animals, and suggest that this would protect brain parenchyma from infiltration by immune cells and ensuing neuroinflammation.

Nicotinamide supplementation prevents microglial activation and mitochondrial impairment middle-aged MS rats

The effects of NAM supplementation on BBB protection led us to postulate that NAM treatment may also forestall the neuroinflammation and mitochondrial dysfunction that emerges in the hippocampi of MS animals in middle-aged life. We noted a significant MS×NAM two-way ANOVA interaction for activated microglial numbers in all hippocampal subfields (Fig. 7b-e), with the increase in activated microglia completely absent in the NAM-administered middle-aged MS cohort. Long-term NAM administration had no effect on activated microglia numbers in control cohorts (Fig. 7b-e). We then addressed the impact of systemic NAM supplementation on hippocampal mitochondrial status, with two-way ANOVA analyses indicating significant MS×NAM interaction effects for SIRT1, PGC-1α , and TFAM expression (Fig. 7f-g), mtDNA content (Fig. 7h), cellular ATP levels (Fig. 7i) and mtROS generation (Fig. 7j). *Post-hoc* group comparison analysis revealed that the MS-evoked decline in SIRT1, PGC-1α and TFAM protein levels, mtDNA content and cellular ATP in the middle-aged MS male rats was completely prevented by NAM supplementation. Similarly, the enhanced hippocampal mtROS production in middle-aged MS male rats was also prevented by NAM treatment. Collectively, we find that long-term NAM supplementation commencing in mature adulthood prevents the impact of MS on peripheral and central inflammatory signatures, BBB integrity, hippocampal mitochondrial health and cognitive performance in middle-aged life (Fig. 8).

Discussion

In this study, we uncover the impact of MS across two major adult life stages, mature adulthood and middle-age. A history of MS led to elevated peripheral biomarkers of inflammation, stress reactivity and aging, compromised neurovascular and blood brain barrier integrity, increased microglial reactivity and disrupted hippocampal mitochondrial health, a brain region central to age-related cognitive outcomes, and impaired object recognition memory in middle-aged life, collectively indicative of premature aging. We find that long-term supplementation with the NAD^+ precursor, NAM, commencing in mature adulthood, prevents many of these late-emerging MS-driven alterations by mitigating peripheral and central inflammation, preserving BBB and neurovascular integrity, maintaining hippocampal mitochondrial health and averting cognitive decline in middle-aged life. Our work provides preclinical evidence linking early-life stress accelerated brain aging to changes in inflammation, neurovascular integrity and mitochondrial health, and shows that adult-onset NAM supplementation can prevent these late emerging alterations.

Previous studies predominantly provide snap-shot measures in young adulthood, and hence there is limited evidence on the temporal emergence of the maladaptive outcomes of early-life stress [8,9,21,22,24,42–48]. Studies with MS and related rodent models of fragmented care indicate varying effects on cognition in adulthood, spanning from no change to transiently adaptive outcomes, to cognitive impairment, varying based on the nature and severity of the stressor [16,17,20,47,49,50]. A few prior studies, with MS in rats and limited bedding and nesting material in mouse models suggest that early-life stress drives cognitive decline in middle-aged life, along with impaired hippocampal synaptic and structural plasticity [13,17,50]. Our results in the MS model indicate a buffering against the damaging effects on object recognition memory until mature adulthood, with marked cognitive decline noted in middle-aged life, supporting the clinical evidence which posits that early adversity accelerates cognitive aging [2,51]. The possibility that the maladaptive trajectory set in motion by MS history remains modifiable [52], is strongly supported by our finding that NAM supplementation prevents the emergence of cognitive decline in middle-aged MS animals of both sexes. While NAD^+ levels are reported to diminish with aging across diverse tissues, including the brain [27], the premature decline in hippocampal NAD^+ levels in middle-aged MS rats is mitigated by NAM supplementation, coinciding with the prevention of cognitive deficits. A prior report using NMR-based metabolomics indicates that MS can disrupt tryptophan-NAD pathway metabolites as early as adolescence and young adulthood [53]. Further, a study with a developmental model of schizophrenia indicates that a month-long NAM treatment in juvenile life offsets cognitive impairments in young adulthood [43]. Amongst the underlying mechanisms postulated for the beneficial effects of NAD^+ precursors on cognitive deficits are reductions in inflammatory load, improvements in metabolic health and support of mitochondrial function [54–56].

Both pre-clinical and clinical studies indicate that early-life stress drives systemic pro-inflammatory alterations noted in postnatal epochs of life, with a paucity of studies addressing changes beyond early adulthood [22,23,49,57]. Middle-aged MS animals of both sexes exhibit elevated levels of diverse pro-inflammatory markers including several cytokines, CRP and kynurenine, alongside aging biomarkers such as GDF15 and methylglyoxal, as well as stress-associated signatures, namely corticosterone, ccf-mtDNA and leukocytosis. Cross-correlational analyses revealed a significant inverse correlation between cognitive performance and circulating levels of GDF15, CRP, IL1ß, IFNγ, TNFα in middle-aged MS, but not control rats, with these changes already detectable in MS animals in mature adulthood, and further worsening with the superimposition of biological aging processes on MS history. These findings point to the persistent reprogramming of stress-responsive systems, immune pathways, and metabolic regulators that remain sensitized long after the cessation of early-life stress, imposing an allostatic load that can shift aging trajectories [26,58]. Amongst these peripheral markers, GDF15 is a putative aging biomarker, that reflects inflammatory status and mitochondrial health, and is thought to hasten cognitive aging [59,60]. Given the frequently modest physiological effects of NAD^+ precursor supplementation in clinical studies of healthy participants [27,61–64], it is likely that the efficacy of NAM supplementation is strongly context-dependent; accordingly, we initiated NAM administration in mature adulthood, coinciding with the first indicators of peripheral inflammatory changes. NAM supplementation significantly

reduced systemic inflammatory load in middle-aged MS animals, with NAM-supplemented MS cohorts indistinguishable from both vehicle and NAM-supplemented controls. In line with clinical reports of reduced peripheral inflammatory burden after NAD^+ precursor supplementation [30,61,62,65], our findings show that NAM reverses the protracted early-life stress effects on systemic inflammation.

Sustained systemic inflammation is tightly linked to neurovascular vulnerability [31–33], and we observed compromised BBB integrity in middle-aged MS animals, but not in mature adulthood. Our findings revealed a clear temporal pattern, with no detectable BBB-associated alterations in mature adulthood, while middle-aged MS animals displayed pronounced BBB disruption. This aligns with prior evidence that MS history can influence endothelial cell function and increase BBB fragility, particularly under inflammatory challenge in adulthood [24]. We observed a distinct pattern of neurovascular dysfunction in the hippocampal parenchyma concurrent with impaired object recognition memory in middle-aged MS animals, which aligns with clinical evidence suggesting that BBB compromise particularly impacts the hippocampus during biological aging and may thus contribute to cognitive deterioration [66]. Further, adult-onset social stressors have also been linked to neurovascular impairments [32], with reports revealing higher systemic sE-selectin concentrations in both animal models of depression and patients with major depressive disorder [33]. Given that our study on enhanced BBB permeability in MS animals was conducted in male rats, the extent to which this particular phenotype generalizes to both sexes remains to be determined. Most strikingly, long-term NAM supplementation initiated in mature adulthood preserved BBB integrity in middle-aged MS animals and normalized accompanying endothelial and inflammatory signatures. Although our findings do not resolve the precise mediators, recent evidence indicating that NAD^+ augmentation supports BBB resilience is consistent with a model in which NAD^+ precursor supplementation protects the BBB, at least in part, by buffering inflammation-driven endothelial dysfunction, via the activation of a Sirt1/FOXO1a pathway [67].

Our findings also reveal that MS history elicits a pronounced neuroinflammatory phenotype in middle-aged life, with alterations in markers of hippocampal inflammatory that were completely absent in mature adulthood. Although it is difficult from our results to parcellate the temporal sequence of these maladaptive consequences in middle-aged life, it is tempting to speculate from our data that they emerge following neurovascular compromise. In this regard it is relevant to note that NAM administration besides mitigating peripheral inflammation and protecting BBB integrity, also prevents the onset of enhanced microglial reactivity within the hippocampi of middle-aged MS animals. The notion that early adversity drives central neuroinflammatory changes is in keeping with reports from other models such as the limited bedding and nesting model, which indicate increased microglial activation in the hippocampus during adulthood under basal and immune-challenged conditions [42,68–71]. These findings point to the fact that the severity of the early-life stress, as well as exposure to secondary hits, may impact both the time-point of onset and magnitude of the deleterious sequelae that ensue.

Early adversity may impose a dual burden by heightening neuroinflammation and simultaneously compromising energy metabolism, creating conditions that promote cognitive

aging [72–75]. In the hippocampus, mitochondrial compromise was not evident in mature adulthood but emerged by middle-age in MS animals, extending prior work that had largely focused on earlier time windows and aligning with limited evidence from related models suggesting later life mitochondrial vulnerability [21,45,76,77]. We find that NAM supplementation protects hippocampal mitochondrial health and restored hippocampal NAD^+ levels, consistent with effects in mitochondrial biogenesis and resilience. Future studies are required to address the impact of NAM supplementation on mitophagy and mitochondrial unfolded protein response, both major processes implicated in aging. The pleiotropic protective effects NAM supplementation reported here suggest that NAM interrupts a mutually reinforcing cycle of inflammation and mitochondrial dysfunction that may otherwise hasten hippocampal dysfunction and cognitive aging triggered by early-stress history.

Prior studies indicate that nutritional supplements, pharmacological modulators, enriched environment and exercise can protect against specific molecular, cellular and behavioural sequelae of early-life stress, with the preponderance of literature focussed on prevention in adulthood [17,44,50,71,78–82]. In addition to the nature of the early-life stressor, the timing of assessment has a major impact on the outcomes, and there are very few studies that have addressed the influence of long-term interventions in preventing the impact of early-life stress on premature aging [17,50]. Studies employing pharmacological strategies, either long-duration antidepressant treatment commencing in mature adulthood or short-term CRH receptor type-1 antagonist treatment in young adults, prevented the cognitive deficits evoked by early adversity in middle-aged life [17,50]. Our results, along with these prior reports, provide support to the notion that biological aging trajectories, in particular those shaped by early-life stress history, remain modifiable. Nutritional gerotherapeutics remain heavily debated as effective tools to extend healthspan, improve physiological function, and reduce vulnerability to age-associated disorders, and results from multiple clinical trials with different NAD^+ precursors reported minimal effects in healthy volunteers [61–65]. Our results uncover differential outcomes, with no effect in middle-aged control cohorts and robust protective actions in MS animals, indicating that the efficacy of NAD^+ precursor treatment may manifest only when health status is compromised and in conditions of NAD^+ deficiency.

In conclusion, we document that early-life stress history progressively tips into maladaptive cognitive impairments concurrent with neurovascular, inflammatory and mitochondrial alterations in the hippocampus later in life. The early signs of premature aging are first noted in mature adulthood with specific systemic inflammaging markers beginning to diverge from controls, with a worsening pattern noted when the ‘second-hit’ of biological aging processes interacts with the vulnerability associated with early stress history. More importantly, our work indicates that these maladaptive consequences are not deterministic, but rather remain amenable to restoration via long-term nutritional supplementation with NAM, raising the possibility of healthspan extension.

Materials and Methods

Animals

Male and female Sprague-Dawley (SD) rats (*Rattus norvegicus*) were bred in the Tata Institute of Fundamental Research (TIFR) animal facility. All animals were group housed and maintained on a 12:12-hour light:dark cycle (lights on at 7:00) with access to food and water *ad libitum*. Animal procedures were in accordance with the Committee for Control and Supervision of Experiments on Animals (CCSEA) guidelines and were approved by the Institutional Animal Ethics Committee (TIFR/IAEC/2019-4). Care was taken across all experiments to minimize animal suffering and restrict the number of animals used.

Animal treatment paradigms

Animals were subjected to the early stress of maternal separation (MS) from postnatal day (P)2 to P14. Litters born to pregnant primiparous dams were assigned randomly to control or MS groups on P1. All experimental litters were chosen to ensure consistency of size of litter ranging from 9 to 11 pups. Pups in the MS group were separated as a litter from their mothers for a period of 3 hours daily (10:00 to 13:00) from P2 to P14. The dams from the MS group were first removed from their home cage to a novel cage prior to the removal of the litter. During this period of daily separation, pups were placed in beakers with bedding and nesting material similar to their home cage and the beakers were placed on temperature controlled heating pads (Flamingo, India) to maintain euthermic conditions. Pups were returned to their home cage at the end of the separation period prior to reinstatement of the dam. Control litters and dams were left undisturbed in their home cage, except for routine animal facility rearing, which involved brief handling during cage cleaning. All the pups, from both control and MS groups, were weaned at P28 and then housed in sex-matched groups of 3 to 4 animals per cage. Subsequent experiments were carried out in both male and female adult progeny from control and MS litters, unless otherwise specified. Control and MS animals were sacrificed either in mature adulthood (6-7 months) or middle-aged life (13-15 months) for further investigations.

Systemic nicotinamide supplementation

We hypothesized that a supplementation of NAD^+ precursor, Nicotinamide (NAM), can mitigate early stress evoked inflammaging. To examine the effect of NAM (#72340, Sigma-Aldrich, USA), 8-month old control and MS rats (males and females) were subjected to NAM administration (100mg/kg/day) in drinking water for a 5-month period, which were designated as CN and MSN respectively. Dose selection was based on prior studies supporting the use of NAD^+ precursors in rodent model [83,84]. Concomitantly, a cohort of control and MS animals of both sexes continued receiving regular drinking water and were assigned as CD and MSD respectively. The bottles were changed every day and animal weights were monitored every 3-4 weeks. Middle-aged control and MS animals (males and females) with or without NAM administration were subjected to object recognition memory task and thereafter sacrificed for further investigations.

Novel object recognition (NOR) task

Control and MS animals of both sexes were assessed on the novel object recognition **(**NOR) task, to assess object recognition memory in mature adulthood (6-7 months) and middle-aged life (13-15 months). Control male animals (22 months) were also assessed on the NOR task to serve as an aged control cohort comparison. Animals were habituated to a novel arena (40 cm × 60 cm × 29 cm) for 3 consecutive days for 20 minutes daily. On day 4, animals were allowed to explore two identical objects in the arena for 15 minutes. Short-term object recognition memory was tested on day 5 by replacing one of the identical objects with a novel object of similar dimensions. On day 10, long-term object recognition memory was assessed by replacing the first novel object with a second novel object, keeping the familiar object constant. Behaviour in the NOR task was scored using an automated tracking system (Noldus Ethovision 3.1, Noldus Information Technology, Netherlands). Discrimination index {[(time spent exploring the novel object - time spent exploring the familiar object) / total object exploration time] X 100} was determined to assess object recognition memory over a 5 minute exploration period. Objects were selected based on a previously published study [17] and pilot experiments performed with a separate cohort of rats to rule out an inherent bias to the objects used in the NOR.

Immunoassays

Control and MS animals (males and females) in mature adulthood (6-7 months) or middle-aged (13-15 months) were sacrificed by rapid decapitation and trunk blood was collected for biochemical measurements. After coagulation of blood at room temperature for 30 minutes, blood samples were centrifuged at 1200 g for 18 minutes in a refrigerated centrifuge (Eppendorf, Germany). Serum collected was aliquoted and stored at -80°C and subsequently used for immunoassays. Baseline circulating levels of inflammatory, aging and stress-associated markers were determined using commercially available enzyme-linked immunosorbent assay (ELISA) kits in accordance with the manufacturer's instructions. The following immunoassays were performed on serum derived from control and MS animals (males and females) in mature adulthood and middle-aged life; growth differentiation factor-15 (GDF15; R & D systems, USA, Cat# MGD150), C-reactive protein (CRP; Invitrogen, USA, Cat# ERCRP), interleukin-1ß (IL1ß; R & D systems, USA, Cat# RLB00), Interferon-γ (IFNγ; R & D systems, USA, Cat# RIF00), Tumor necrosis factor-α (TNFα; R & D systems, USA, Cat# RTA00), IL10 (R & D systems, USA, Cat# R1000), IL4 (R & D systems, USA, Cat# R4000), IL6 (Invitrogen, USA, Cat# ERA31RB), IL18 (Invitrogen, USA, Cat# KRC2341), methylglyoxal (MG; Cell biolabs, USA, Cat# STA-811), kynurenine (My biosource, USA, Cat# MBS7607149), E-selectin (Invitrogen, USA, Cat# ERA14RB), nicotinamide phosphoribosyltransferase (NAMPT; Adipogen life sciences, Switzerland, Cat#AG-45A-0007YTP-KI01). The optical density was determined at 450 nm on a microplate reader (Tecan life sciences, Switzerland, Cat# Infinite M200 Pro). Further, levels of corticosterone (R & D systems, USA, KGE009) were evaluated using serum samples as per manufacturer's guidelines. All serum samples used for immunoassays were tested in duplicate. Concomitantly, blood samples were collected in dipotassium ethylenediaminetetraacetic acid (K2-EDTA) tubes (Dr. Bloodo, India) and assessed for complete blood count (CBC) at Shahbazker's Diagnostic Centre, Mumbai, India. IFNγ levels in the hippocampal homogenates of control and

MS male rats were evaluated using commercially available ELISA kit (R & D systems, Cat# RIF00) in accordance with the manufacturer's instructions. For those samples used for cross-correlational analyses with NOR behaviour, animals were first subjected to the NOR task following which they were euthanized to collect blood for biochemical investigations.

Quantitative Real-Time Polymerase Chain Reaction (qPCR)

Hippocampal tissue was homogenized in a TRIzol reagent (Sigma-Aldrich, USA, Cat# 15596018) and subjected to RNA extraction. RNA (1000 ng) was reverse transcribed using the PrimeScript RT reagent kit (Takara Bio, Japan, Cat# RR037A). cDNA was subjected to qPCR using the CFX96 qRT-PCR system (Bio-Rad, USA) in 96-well PCR plate (Bio-rad, USA, Cat# HSP-9601). Primers for the genes of interest were designed using National Center for Biotechnology Information (NCBI) primer designing tool. Data analysis was performed using $^{\Delta\Delta}$Ct method [85] and normalized against the 18S rRNA (18S) gene. The list of primer sequences is provided in supplementary information (Source data 1).

Circulating cell free mitochondrial DNA (ccf-mtDNA) quantification

Circulating cell free mitochondrial DNA **(**ccf-mtDNA) quantitation was carried out using the MitoQuicLy method [86]. Serum was incubated with lysis buffer consisting of Tween-20 (6%, Sigma-Aldrich, USA, Cat#11332465001), Tris-HCl (pH 8.5, 114 mM, Himedia, India, Cat# MB030) and Proteinase K (200 µg/mL, Invitrogen, USA, Cat #25530049) in a 96-well PCR plate overnight at 55°C for 16 hours in a thermocycler (Eppendorf, Germany, Cat# Mastercycler nexus), followed by Proteinase K inactivation at 95°C for 10 minutes. qPCR was performed using this lysate on the CFX96 qRT-PCR system (Bio-Rad, USA) for a mitochondrial genome-encoded gene (cytochrome b, *Cytb*) and a nuclear genome-encoded gene (cytochrome c, *Cycs*) in 96-well PCR plate (Bio-rad, USA, Cat# HSP-9601). *Cycs* data were normalized to *Cytb*, and quantified by $^{\Delta\Delta}$Ct method to determine relative ccf-mtDNA levels between the groups. The primer sequences used are provided in the supplementary file (Source data 1).

Blood brain barrier integrity assay

Integrity of the blood brain barrier (BBB) was assessed using an Evans blue extravasation assay [87,88]. Evans blue (EB) dye (2%, Sigma-Aldrich, USA, Cat# E2129) was slowly injected through the tail vein of control and MS male rats, and animals were perfused with saline 20 hours post injection to remove intravascular blood containing EB. Hippocampal tissue was homogenized in phosphate-buffered saline (PBS) followed by a centrifuge at 10000 g for 20 minutes. The supernatant was incubated overnight with 50% trichloroacetic acid (TCA, Sigma-Aldrich, USA, Cat# T0699) solution (1:2 ratio) with gentle rocking to extract extravasated EB. Following a centrifugation at 10000 g, fluorescence was measured on a microplate reader (Tecan life sciences, Switzerland). The intensities were normalized to hippocampal tissue weight. Liver was assessed as a positive control. BBB integrity was also determined using micro-SPECT (Single Photon Emission Computed Tomography) imaging (Gamma Eye, Bioemtech, Greece) [89]. The radiotracer 99mTc (200 µCi/100 µl) was injected through the tail vein of control and MS male animals and one hour post-injection the brain was harvested for

ex vivo SPECT scanning. Reconstructed images were analyzed using visual eye software (Bioemtech, Greece) and plotted as 99mTc radioactivity counts. Thyroid gland was analyzed as a positive control.

Western blotting

Hippocampal tissue was homogenized in Radioimmunoprecipitation assay (RIPA) buffer: Tris-Cl (pH 8.0, 10 mM), Ethylenediamine tetraacetic acid (EDTA; 1 mM), Ethylene glycol tetraacetic acid (EGTA; 0.5 mM), Triton X-100 (1%), sodium deoxycholate (0.1%), sodium dodecyl sulphate (SDS; 0.1%), sodium chloride (NaCl; 140 mM) containing protease and phosphatase inhibitors (Sigma-Aldrich, USA) using a dounce homogenizer (Sigma-Aldrich, USA). Protein estimation was performed using a Quantipro BCA assay kit (Sigma-Aldrich, USA, Cat# QPBCA). Protein lysates (20-90 µg) were resolved using 8-13.5% SDS polyacrylamide gel electrophoresis system (Bio-rad, USA) and transferred onto polyvinylidene fluoride (PVDF) membranes (Merck Millipore, Germany, Cat# IPVH00010). Blots were stained with Ponceue-S (Sigma-Aldrich, USA, Cat# 3504) to confirm efficient transfer and destained with tris-buffered saline containing Tween-20 (TBST). Further, blots were subjected to blocking with either non-fat dry milk (5%) or bovine serum albumin (BSA; 5%) prepared in TBST for 1 hour and incubated overnight on a refrigerated rocker with primary antibodies prepared in a blocking solution. Following antibodies were used in this study: rabbit anti-SIRT1 (1:1000, Cat# 07-131, Millipore, USA), mouse anti-PGC-1α (1:500, Calbiochem, Germany, Cat# KP9803), rabbit anti-TFAM (1:2000, Abcam, UK, Cat# ab131607), rabbit anti NF-κB p65 (1:2000, Cell signaling technology, USA, Cat# 8242), rabbit anti-NLRP3 (1:500, Novus biologicals, USA, Cat# NBP2-12446), rabbit anti-ASC (1:500, Santa Cruz Biotechnology, USA, Cat# sc-22514-R). Rabbit anti-β-Actin (1:12000, Abclonal technology, USA, Cat# AC026) was used as a protein loading control for normalization. Following washes with TBST, blots were incubated with HRP-conjugated goat anti-rabbit secondary antibody (1:8000, Abclonal Technology, USA, Cat# AS014) or HRP-conjugated goat anti-mouse secondary antibody (1:8000, AS003, Abclonal Technology) for 1 hour. The blots were washed with TBST and signal was visualized on a GE Amersham Imager 800 (GE life sciences, USA) with a western blotting chemiluminescent detection kit (Advansta, USA, Cat# K-12045-D20). Densitometric quantitative analysis was performed using ImageJ (National Institutes of Health, USA) software. Unprocessed blots are provided in the supplementary file (Source data 2).

Immunohistochemical and cell counting analysis

Animals were transcardially perfused with ice-cold 0.9% saline (Sodium chloride, MP Biomedicals, India, Cat# 194848,) followed by ice-cold paraformaldehyde (4%, PFA, MP Biomedicals, India, Cat# 150146). Brains were harvested and fixed in PFA (4%) for 48 hours prior to generating serial coronal sections (50 µm) on a vibratome (Leica Microsystems, Germany, Cat# VT1000 S) and stored in 0.1M phosphate buffer, pH 7.4 (PB; di-Sodium hydrogen phosphate dihydrate, Merck Millipore, USA, Cat# 106580, Sodium dihydrogen phosphate dihydrate, Merck Millipore, USA, Cat# 106342) containing 0.1% sodium azide (MP Biomedicals, India, Cat# 102891). Activation of microglia in the hippocampus was assessed by performing immunofluorescence experiment for Ionized calcium binding adaptor molecule

1 (Iba1), a microglial marker. Hippocampal sections (6 sections per animal, n = 5-6 males per group) were permeabilized with 0.1M PB containing 0.3% Triton X-100 (0.3% PBTx) for 30 minutes followed by blocking with horse serum (10%; Thermo Fisher Scientific, USA, Cat# 26-050-088) prepared in 0.3% PBTx, for 2 hours at room temperature. The sections were then incubated with goat anti-Iba1 (1:1000, Abcam, UK, Cat# ab5076) overnight at room temperature. Following subsequent serial washes with 0.1M PB, sections were incubated with a secondary antibody, Alexa Fluor 568-conjugated donkey anti-goat IgG (1:400, Thermo Fisher Scientific, USA, Cat# A11057) for 3 hours at room temperature. After serial washes with 0.1M PB, sections were mounted on cleaned glass slides using Vectashield antifade mounting medium with 4',6-diamidino-2-phenylindole (Vector Laboratories, USA, Cat# H-1200) and visualized under the Zeiss LSM 5 Exciter confocal microscope (Zeiss, Germany). Cell counting analysis was performed by an experimenter blind to the treatment conditions. Iba1-positive cells were manually counted as activated or resting state microglia based on morphological characteristics of these microglial states in all the hippocampal subfields. Counting was performed in a region of interest (ROI) representing dimensions of 1388 x 1040 pixels per subfield in six sections, at a periodicity of every sixth section spanning the rostro-caudal extent of the hippocampus (Bregma −3.30 to −5.80) using the Zeiss LSM 5 Exciter confocal microscope camera (Zeiss, Germany) at a magnification of 200X. Data are represented as the number of activated microglia per mm^2 area in each hippocampal subfield. Representative images were acquired on a FV3000 confocal microscope (Olympus, Japan).

Mitochondrial DNA measurement

Total genomic DNA was extracted from the hippocampi of control and MS animals using a Purelink genomic DNA mini kit (Thermo Fisher Scientific, USA, Cat# K182002). qPCR was performed on the CFX96 qRT-PCR system (Bio-Rad, USA) for a mitochondrial genome-encoded gene (cytochrome b, *Cytb*) and a nuclear genome-encoded gene (cytochrome c, *Cycs*) in 96-well PCR plate (Bio-rad, USA, Cat# HSP-9601). Data were normalized to *Cycs*, and quantified by $^{\Delta\Delta}$Ct method. The primer sequences used are provided in the supporting information (Source data 1).

Isolation of mitochondria and bioenergetic measurements

The mitochondrial state respiration assay was conducted by measuring the oxygen consumption rate (OCR) in isolated mitochondria derived from middle-aged control and MS hippocampi using the Seahorse XFe24 Analyzer (Agilent, USA), as per the manufacturer's instructions. Hippocampi were homogenized in ice-cold mitochondrial isolation buffer (MSHE+BSA, pH 7.2), containing mannitol (210 mM), sucrose (70 mM), (N-(2-Hydroxyethyl) Piperazine-N(2-Ethane Sulphonic Acid) HEPES (5 mM), EGTA (1 mM), and fatty acid-free BSA (0.5%) using a Dounce homogenizer (6 strokes). Following refrigerated centrifugation at 800 g for 10 minutes, the supernatant was collected in a separate tube and centrifuged at 8000 g for 10 minutes at 4°C. The pellet was suspended in MSHE+BSA, and the centrifugation procedure was repeated. Finally, the pellet was resuspended in a small volume of ice-cold mitochondrial assay buffer (MAS+BSA, pH 7.2), containing mannitol (220 mM), sucrose (70 mM), potassium dihydrogen phosphate (KH_2PO_4, 10 mM), magnesium

chloride ($MgCl_2$, 5 mM), HEPES (2 mM), EGTA (1 mM) and fatty acid-free BSA (0.5%). Protein estimation was performed using a Quantipro BCA assay kit (Sigma-Aldrich, USA, Cat# QPBCA). The mitochondrial suspension (20 µg) was used for bioenergetic analysis immediately after isolation and protein estimation. Mitochondria were plated (20 µg / 50 µl) in Seahorse XFe24 micro-plates (Agilent, USA, Cat# 100850-001) in MAS+BSA buffer supplemented with substrates, pyruvate (10 mM) and malate (2 mM), and centrifuged at 2000 g for 20 minutes at 4°C. Concomitantly, substrate containing MAS+BSA (450 µl) was added to each well. Basal state-2 respiration, primarily Complex-I dependent, under limiting endogenous ADP and succinate concentrations, was measured initially. Following this, Complex-II dependent state-3 respiration was measured post injection of rotenone (2 µM)+ Succinate (10 mM) + Adenosine diphosphate (ADP; 4 mM). Oligomycin (2 µM) induced state-4 respiration was measured next, which was followed by Carbonyl cyanide 4-(trifluoromethoxy)phenylhydrazone (FCCP, 8 µM) induced maximal respiration and non-mitochondrial respiration following antimycin A (8 µM) injections.

Mitochondrial reactive oxygen species (ROS) assay

Mitochondria were isolated from hippocampus of mature adult and middle-aged control and MS male rats. The isolated mitochondrial suspension was diluted to 5 µg/12.5 µl of MAS buffer. 4X Substrate mixture (succinate and rotenone; 25 µL) was added to each well. Amplex red (Sigma-Aldrich, USA, Cat# A36006) was diluted to 400 µM and mixed 1:1 with the mitochondrial suspension, and 25 µl of this mixture was added to each well. Fresh 20 mM hydrogen peroxide (H_2O_2) was prepared by adding 11.5 µl of H_2O_2 (3%) to 988.5 µl of MAS buffer for standard ROS measurements. A working standard was prepared by adding 0.5 µl of H_2O_2 (20 mM) stock and 10 µl amplex red (10 mM) to 989.5 µl of MAS buffer. Serial dilutions of this cocktail were added to standard wells and adjusted to 50 ul volume using MAS buffer. 50 ul Horse Radish Peroxidase (HRP; 20 U/ml) to each well for a total reaction volume of 100 µl. Fluorescence was measured using a black 96-well plate (Thermo Scientific, USA) on a microplate reader (Infinite 200 Pro, Tecan life sciences, Switzerland) at 530 nm excitation and 590 nm emission every 5 minutes for 1 hour or until the standards saturated.

Cellular ATP measurement

Hippocampal tissue from control and MS rats (males and females) was lysed in boiling water and lysate was centrifuged at 12000 rpm for 20 minutes at 4°C. The ATP levels in the supernatant were quantified using the ATP bioluminescent assay kit (Sigma-Aldrich, USA, Cat# FLAA), by mixing the luciferin substrate and luciferase enzyme mix with equal amounts of supernatant in a 96-well black plate. The light emitted is proportional to the ATP consumed in the reaction, and was measured using a luminometer (Berthold technologies, Germany). Cellular ATP levels were normalized to the total protein content of tissue which was estimated using a Quantipro BCA protein assay kit (Sigma-Aldrich, USA, Cat# QPBCA).

Measurement of nicotinamide adenine dinucleotide (NAD^+) levels

NAD^+ levels from hippocampus of control and MS animals (males and females) were evaluated immediately post tissue harvesting using the NAD/NADH quantitation kit (Sigma-Aldrich,

USA, Cat# MAK037) according to the manufacturer's instructions. NAD^+ levels were normalized to protein content of hippocampal tissue, estimated using a BCA protein assay kit (Sigma-Aldrich, USA, Cat# QPBCA).

Data representation and statistical analyses

All data were assessed for normal distribution using the Kolmogorov-Smirnov test on GraphPad Prism 10 (Graphpad Software Inc, USA) prior to performing appropriate statistical testing. For statistical analysis on experiments with two groups that followed a normal distribution, a two-tailed, unpaired Student's *t*-test was performed. Welch's corrections were applied in those instances where there was a significant difference in the variances between groups. For experiments where the data did not follow a normal distribution, the Mann-Whitney-U-test was used for group comparisons. For statistical analyses of experiments with three groups, one-way analysis of variance (ANOVA) analysis was performed, followed by Tukey's *post-hoc* comparison test when the one-way ANOVA results were significant. For statistical analyses of experiments with four groups and two variables, two-way ANOVA analysis was performed, followed by Tukey's *post-hoc* comparison test when a significant interaction ($p < 0.05$) was noted between the variables of the early-life stress of MS and adult-onset NAM supplementation. Data are represented as mean ± standard error of mean (SEM). As we did not observe any significant sex differences in the behavioural, molecular and cellular measures in MS animals, results represented combined data from both male and female rats. Specific measures were performed only in male rats which is indicated in the results. The dots in graphical representations depict individual animals in each experiment, with the lighter shade used for males and darker shade for females. Graphs, heatmaps and correlation matrices were generated using GraphPad Prism 10 software. For gene expression data, false discovery rate (FDR) analysis was carried out using the Benjamini-Hochberg method, and these are denoted as FDR-corrected *p* values. For correlational analyses, Pearson's correlation coefficient (r) was calculated using GraphPad Prism 10 software. Statistical significance was determined at $p \leq 0.05$. The details of statistical analyses are provided in the supporting information (Source data 3, Source data 4).

Acknowledgments

We dedicate this work to the exemplary mentorship of the late Dr. Ashok D.B. Vaidya. P.R.C. acknowledges funding support from India Alliance (Department of Biotechnology, India and Wellcome Trust, United Kingdom) Early Career Fellowship (Reference No. IA/E/18/1/504310). V.A.V. acknowledges funding support from Department of Atomic Energy to Tata Institute of Fundamental Research (Reference No. RTI4003), Sree Ramakrishna Paramahamsa Research Grant from the Sree Padmavathi Venkateswara Foundation (Reference No. SreePVF/G/BS/19/1) and JC Bose Fellowship from Anusandhan National Research Foundation (Reference No. JCB/2021/000014). We thank the animal house staff as well as Dr. Ankit Sood, Vani Dewan, Souparno Das, Dr. Amogh BJ, Dr. Pankaj Kumar at TIFR, Mumbai, India and Dr. Haissa De Castro Abrantes at EPFL, Lausanne, Switzerland for their technical assistance. The schematic representations used in the figures and extended data were created using BioRender.com.

References

1. Nelson, C. A. *et al.* Adversity in childhood is linked to mental and physical health throughout life. *BMJ* **371**, (2020).
2. Künzi, M., Gheorghe, D. A., Gallacher, J. & Bauermeister, S. The impact of early adversity on later life health, lifestyle, and cognition. *BMC Public Health* **24**, (2024).
3. Sapolsky, R. Making sense of the costs of adversity throughout the lifespan on aging in humans and other animals. *Neurosci. Biobehav. Rev.* **159**, (2024).
4. Nelson, C. A., Sullivan, E. F. & Valdes, V. Early adversity alters brain architecture and increases susceptibility to mental health disorders. *Nat. Rev. Neurosci.* **26**, 642–656 (2025).
5. Birnie, M. T. & Baram, T. Z. The evolving neurobiology of early-life stress. *Neuron* **113**, 1474–1490 (2025).
6. Yajima, H. *et al.* Early-life stress induces cognitive disorder in middle-aged mice. *Neurobiol. Aging* **64**, 139–146 (2018).
7. Epel, E. S. & Prather, A. A. Stress, Telomeres, and Psychopathology: Toward a Deeper Understanding of a Triad of Early Aging. *Annu. Rev. Clin. Psychol.* **14**, 371–397 (2018).
8. Chaudhari, P. R., Singla, A. & Vaidya, V. A. Early Adversity and Accelerated Brain Aging: A Mini-Review. *Front. Mol. Neurosci.* **15**, (2022).
9. Chen, Y. & Baram, T. Z. Toward Understanding How Early-Life Stress Reprograms Cognitive and Emotional Brain Networks. *Neuropsychopharmacology* **41**, 197–206 (2016).
10. Yam, K. Y., Naninck, E. F. G., Schmidt, M. V., Lucassen, P. J. & Korosi, A. Early-life adversity programs emotional functions and the neuroendocrine stress system: the contribution of nutrition, metabolic hormones and epigenetic mechanisms. *Stress* **18**, 328–342 (2015).
11. Rice, C. J., Sandman, C. A., Lenjavi, M. R. & Baram, T. Z. A novel mouse model for acute and long-lasting consequences of early life stress. *Endocrinology* **149**, 4892–4900 (2008).
12. Wang, D., Levine, J. L. S., Avila-Quintero, V., Bloch, M. & Kaffman, A. Systematic review and meta-analysis: effects of maternal separation on anxiety-like behavior in rodents. *Transl. Psychiatry* **10**, (2020).
13. Walker, C. D. *et al.* Chronic early life stress induced by limited bedding and nesting (LBN) material in rodents: critical considerations of methodology, outcomes and translational potential. *Stress* **20**, 421–448 (2017).
14. Wendel, K. M. *et al.* Early life adversity in male mice sculpts reward circuits. *Neurobiol. Stress* **15**, (2021).
15. Aisa, B., Tordera, R., Lasheras, B., Del Río, J. & Ramírez, M. J. Cognitive impairment associated to HPA axis hyperactivity after maternal separation in rats. *Psychoneuroendocrinology* **32**, 256–266 (2007).
16. Suri, D., Bhattacharya, A. & Vaidya, V. A. Early stress evokes temporally distinct consequences on the hippocampal transcriptome, anxiety and cognitive behaviour. *Int. J. Neuropsychopharmacol.* **17**, 289–301 (2014).
17. Suri, D. *et al.* Early stress evokes age-dependent biphasic changes in hippocampal neurogenesis, BDNF expression, and cognition. *Biol. Psychiatry* **73**, 658–666 (2013).
18. Tzanoulinou, S. & Sandi, C. The Programming of the Social Brain by Stress During Childhood and Adolescence: From Rodents to Humans. *Curr. Top. Behav. Neurosci.* **30**, 411–429 (2017).

19. Birnie, M. T. *et al.* Plasticity of the Reward Circuitry After Early-Life Adversity: Mechanisms and Significance. *Biol. Psychiatry* **87**, 875–884 (2020).
20. Kotah, J. M., Hoeijmakers, L., Nutma, E., Lucassen, P. J. & Korosi, A. Early-life stress does not alter spatial memory performance, hippocampal neurogenesis, neuroinflammation, or telomere length in 20-month-old male mice. *Neurobiol. Stress* **15**, (2021).
21. Ruigrok, S. R. *et al.* Effects of early-life stress on peripheral and central mitochondria in male mice across ages. *Psychoneuroendocrinology* **132**, (2021).
22. Dutcher, E. G. *et al.* Early-life stress and inflammation: A systematic review of a key experimental approach in rodents. *Brain Neurosci. Adv.* **4**, 239821282097804 (2020).
23. Chen, M. A. *et al.* Immune and Epigenetic Pathways Linking Childhood Adversity and Health Across the Lifespan. *Front. Psychol.* **12**, (2021).
24. Solarz, A., Majcher-Maślanka, I., Kryst, J. & Chocyk, A. Early-life stress affects peripheral, blood-brain barrier, and brain responses to immune challenge in juvenile and adult rats. *Brain Behav. Immun.* **108**, 1–15 (2023).
25. Kim, J. J. & Diamond, D. M. The stressed hippocampus, synaptic plasticity and lost memories. *Nat. Rev. Neurosci.* **3**, 453–462 (2002).
26. McEwen, B. S. Sex, stress and the hippocampus: Allostasis, allostatic load and the aging process. *Neurobiol. Aging* **23**, 921–939 (2002).
27. Xie, N. *et al.* NAD+ metabolism: pathophysiologic mechanisms and therapeutic potential. *Signal Transduct. Target. Ther.* **5**, (2020).
28. Otmani, A., Jóhannesson, G., Brautaset, R., Tribble, J. R. & Williams, P. A. Prophylactic nicotinamide treatment protects from rotenone-induced neurodegeneration by increasing mitochondrial content and volume. *Acta Neuropathol. Commun.* **12**, (2024).
29. Stevens, M. J. *et al.* Nicotinamide reverses neurological and neurovascular deficits in streptozotocin diabetic rats. *J. Pharmacol. Exp. Ther.* **320**, 458–464 (2007).
30. Ungerstedt, J. S., Blombäck, M. & Söderström, T. Nicotinamide is a potent inhibitor of proinflammatory cytokines. *Clin. Exp. Immunol.* **131**, 48–52 (2003).
31. Galea, I. The blood-brain barrier in systemic infection and inflammation. *Cell. Mol. Immunol.* **18**, 2489–2501 (2021).
32. Menard, C. *et al.* Social stress induces neurovascular pathology promoting depression. *Nat. Neurosci.* **20**, 1752–1760 (2017).
33. Dion-Albert, L. *et al.* Vascular and blood-brain barrier-related changes underlie stress responses and resilience in female mice and depression in human tissue. *Nat. Commun.* **13**, (2022).
34. Zhang, J., Huang, S., Zhu, Z., Gatt, A. & Liu, J. E-selectin in vascular pathophysiology. *Front. Immunol.* **15**, (2024).
35. Bonney, S. *et al.* Gamma Interferon Alters Junctional Integrity via Rho Kinase, Resulting in Blood-Brain Barrier Leakage in Experimental Viral Encephalitis. *mBio* **10**, (2019).
36. Trinchese, G., Cimmino, F., Catapano, A., Cavaliere, G. & Mollica, M. P. Mitochondria: the gatekeepers between metabolism and immunity. *Front. Immunol.* **15**, (2024).
37. Picard, M., McEwen, B. S., Epel, E. S. & Sandi, C. An energetic view of stress: Focus on mitochondria. *Front. Neuroendocrinol.* **49**, 72–85 (2018).
38. Weger, M. *et al.* Mitochondrial gene signature in the prefrontal cortex for differential susceptibility to chronic stress. *Sci. Rep.* **10**, (2020).

39. Hoffmann, A. & Spengler, D. The Mitochondrion as Potential Interface in Early-Life Stress Brain Programming. *Front. Behav. Neurosci.* **12**, (2018).
40. Souder, D. C. *et al.* Neuron-specific isoform of PGC-1α regulates neuronal metabolism and brain aging. *Nat. Commun.* **16**, (2025).
41. Lo Iacono, L. *et al.* Adversity in childhood and depression: linked through SIRT1. *Transl. Psychiatry* **5**, (2015).
42. Reemst, K. *et al.* Early-life stress lastingly impacts microglial transcriptome and function under basal and immune-challenged conditions. *Transl. Psychiatry* **12**, (2022).
43. Hao, K. *et al.* Nicotinamide reverses deficits in puberty-born neurons and cognitive function after maternal separation. *J. Neuroinflammation* **19**, (2022).
44. Cui, M. *et al.* Enriched environment experience overcomes the memory deficits and depressive-like behavior induced by early life stress. *Neurosci. Lett.* **404**, 208–212 (2006).
45. Vlaikou, A. M. *et al.* Early Life Stress Induces Brain Mitochondrial Dynamics Changes and Sex-Specific Adverse Effects in Adulthood. *J. Neurosci. Res.* **103**, (2025).
46. Sierra-Fonseca, J. A. *et al.* Neonatal Maternal Separation Modifies Proteostasis Marker Expression in the Adult Hippocampus. *Front. Mol. Neurosci.* **14**, (2021).
47. Alves, J., de Sá Couto-Pereira, N., de Lima, R. M. S., Quillfeldt, J. A. & Dalmaz, C. Effects of Early Life Adversities upon Memory Processes and Cognition in Rodent Models. *Neuroscience* **497**, 282–307 (2022).
48. Endo, N. *et al.* The effects of maternal separation on behaviours under social-housing environments in adult male C57BL/6 mice. *Sci. Rep.* **11**, (2021).
49. Cruz-Pereira, J. S. *et al.* Depression's Unholy Trinity: Dysregulated Stress, Immunity, and the Microbiome. *Annu. Rev. Psychol.* **71**, 49–78 (2020).
50. Short, A. K., Maras, P. M., Pham, A. L., Ivy, A. S. & Baram, T. Z. Blocking CRH receptors in adults mitigates age-related memory impairments provoked by early-life adversity. *Neuropsychopharmacology* **45**, 515–523 (2020).
51. Joshi, A. & Yeo, J. The Role of Childhood Adversity and Social Drivers of Health in Subjective Cognitive Decline. *Prev. Chronic Dis.* **22**, (2025).
52. Dohm-Hansen, S. *et al.* The 'middle-aging' brain. *Trends Neurosci.* **47**, 259–272 (2024).
53. Tomassini, A. *et al.* 1H NMR-based urinary metabolic profiling reveals changes in nicotinamide pathway intermediates due to postnatal stress model in rat. *J. Proteome Res.* **13**, 5848–5859 (2014).
54. Hao, K. *et al.* Cognitive impairment following maternal separation in rats mediated by the NAD+/SIRT3 axis via modulation of hippocampal synaptic plasticity. *Transl. Psychiatry* **15**, (2025).
55. Qader, M. A. *et al.* A systematic review of the therapeutic potential of nicotinamide adenine dinucleotide precursors for cognitive diseases in preclinical rodent models. *BMC Neurosci.* **26**, (2025).
56. Zhao, Y. *et al.* NAD+ improves cognitive function and reduces neuroinflammation by ameliorating mitochondrial damage and decreasing ROS production in chronic cerebral hypoperfusion models through Sirt1/PGC-1α pathway. *J. Neuroinflammation* **18**, (2021).
57. Pedersen, J. M. *et al.* Prenatal and early postnatal stress and later life inflammation. *Psychoneuroendocrinology* **88**, 158–166 (2018).

58. Bobba-Alves, N. *et al.* Cellular allostatic load is linked to increased energy expenditure and accelerated biological aging. *Psychoneuroendocrinology* **155**, (2023).
59. Liu, C. C., Trumpff, C., Huang, Q., Juster, R. P. & Picard, M. Biopsychosocial correlates of resting and stress-reactive salivary GDF15: preliminary findings. *Brain Behav. Immun.* **130**, (2025).
60. Jiang, J., Wen, W. & Sachdev, P. S. Macrophage inhibitory cytokine-1/growth differentiation factor 15 as a marker of cognitive ageing and dementia. *Curr. Opin. Psychiatry* **29**, 181–186 (2016).
61. Damgaard, M. V. & Treebak, J. T. What is really known about the effects of nicotinamide riboside supplementation in humans. *Sci. Adv.* **9**, (2023).
62. Kang, B. E., Choi, J. Y., Stein, S. & Ryu, D. Implications of NAD+ boosters in translational medicine. *Eur. J. Clin. Invest.* **50**, (2020).
63. Xu, P. & Sauve, A. A. Vitamin B3, the nicotinamide adenine dinucleotides and aging. *Mech. Ageing Dev.* **131**, 287–298 (2010).
64. Poljšak, B., Kovač, V., Špalj, S. & Milisav, I. The Central Role of the NAD+ Molecule in the Development of Aging and the Prevention of Chronic Age-Related Diseases: Strategies for NAD+ Modulation. *Int. J. Mol. Sci.* **24**, (2023).
65. Qader, M. A. *et al.* A systematic review of the therapeutic potential of nicotinamide adenine dinucleotide precursors for cognitive diseases in preclinical rodent models. *BMC Neurosci.* **26**, (2025).
66. Montagne, A. *et al.* Blood-brain barrier breakdown in the aging human hippocampus. *Neuron* **85**, 296–302 (2015).
67. Liu, R. *et al.* Nicotinamide mononucleotide rescues Di-n-butyl phthalate induced blood-brain barrier damage via NAD+/Sirt1/FOXO1a pathway activation. *Ecotoxicol. Environ. Saf.* **305**, (2025).
68. Bolton, J. L. *et al.* Early stress-induced impaired microglial pruning of excitatory synapses on immature CRH-expressing neurons provokes aberrant adult stress responses. *Cell Rep.* **38**, (2022).
69. Jiang, S. *et al.* Intra-individual methylomics detects the impact of early-life adversity. *Life Sci. Alliance* **2**, (2019).
70. Reemst, K. *et al.* Early-life stress and dietary fatty acids impact the brain lipid/oxylipin profile into adulthood, basally and in response to LPS. *Front. Immunol.* **13**, (2022).
71. Ruigrok, S. R. *et al.* Effects of Early-Life Stress, Postnatal Diet Modulation and Long-Term Western-Style Diet on Peripheral and Central Inflammatory Markers. *Nutrients* **13**, 1–21 (2021).
72. Hendricks, S., Ojuka, E., Kellaway, L. A., Mabandla, M. V. & Russell, V. A. Effect of maternal separation on mitochondrial function and role of exercise in a rat model of Parkinson's disease. *Metab. Brain Dis.* **27**, 387–392 (2012).
73. Picca, A. *et al.* Mitochondrial Dysfunction, Oxidative Stress, and Neuroinflammation: Intertwined Roads to Neurodegeneration. *Antioxidants (Basel).* **9**, 1–21 (2020).
74. Picard, M., Juster, R. P. & McEwen, B. S. Mitochondrial allostatic load puts the 'gluc' back in glucocorticoids. *Nat. Rev. Endocrinol.* **10**, 303–310 (2014).
75. Kumsta, R. The role of stress in the biological embedding of experience. *Psychoneuroendocrinology* **156**, (2023).
76. Hofstra, B. M., Hoeksema, E. E., Kas, M. J. & Verbeek, D. S. Cross-species analysis uncovers the mitochondrial stress response in the hippocampus as a shared mechanism in mouse early life stress and human depression. *Neurobiol. Stress* **31**, (2024).

77. Zhang, S. *et al.* Activation of RXRα mitigates maternal separation-induced hippocampal neurodevelopmental impairment in mice by inhibiting oxidative stress and restoring mitochondrial homeostasis. *Free Radic. Biol. Med.* **243**, 507–521 (2026).
78. Naninck, E. F. G. *et al.* Early micronutrient supplementation protects against early stress-induced cognitive impairments. *FASEB J.* **31**, 505–518 (2017).
79. Geertsema, J. *et al.* Nutritional interventions to counteract the detrimental consequences of early-life stress. *Mol. Psychiatry* **30**, 3269–3300 (2025).
80. Donoso, F. *et al.* Polyphenols selectively reverse early-life stress-induced behavioural, neurochemical and microbiota changes in the rat. *Psychoneuroendocrinology* **116**, (2020).
81. O'Mahony, S. M. *et al.* The enduring effects of early-life stress on the microbiota-gut-brain axis are buffered by dietary supplementation with milk fat globule membrane and a prebiotic blend. *Eur. J. Neurosci.* **51**, 1042–1058 (2020).
82. Ivy, A. S. *et al.* Hippocampal dysfunction and cognitive impairments provoked by chronic early-life stress involve excessive activation of CRH receptors. *J. Neurosci.* **30**, 13005–13015 (2010).
83. Yang, S. J. *et al.* Nicotinamide improves glucose metabolism and affects the hepatic NAD-sirtuin pathway in a rodent model of obesity and type 2 diabetes. *J. Nutr. Biochem.* **25**, 66–72 (2014).
84. Morató, L. *et al.* eNAMPT actions through nucleus accumbens NAD+/SIRT1 link increased adiposity with sociability deficits programmed by peripuberty stress. *Sci. Adv.* **8**, (2022).
85. Bookout, A. L. & Mangelsdorf, D. J. Quantitative real-time PCR protocol for analysis of nuclear receptor signaling pathways. *Nucl. Recept. Signal.* **1**, nrs.01012 (2003).
86. Michelson, J. *et al.* MitoQuicLy: A high-throughput method for quantifying cell-free DNA from human plasma, serum, and saliva. *Mitochondrion* **71**, 26–39 (2023).
87. Wang, H. L. & Lai, T. W. Optimization of Evans blue quantitation in limited rat tissue samples. *Sci. Rep.* **4**, (2014).
88. Goldim, M. P. de S., Della Giustina, A. & Petronilho, F. Using Evans Blue Dye to Determine Blood-Brain Barrier Integrity in Rodents. *Curr. Protoc. Immunol.* **126**, (2019).
89. Kumar, P. *et al.* Radiolabeling and preclinical evaluation of technetium-99m labeled colistin. *Appl. Radiat. Isot.* **214**, (2024).

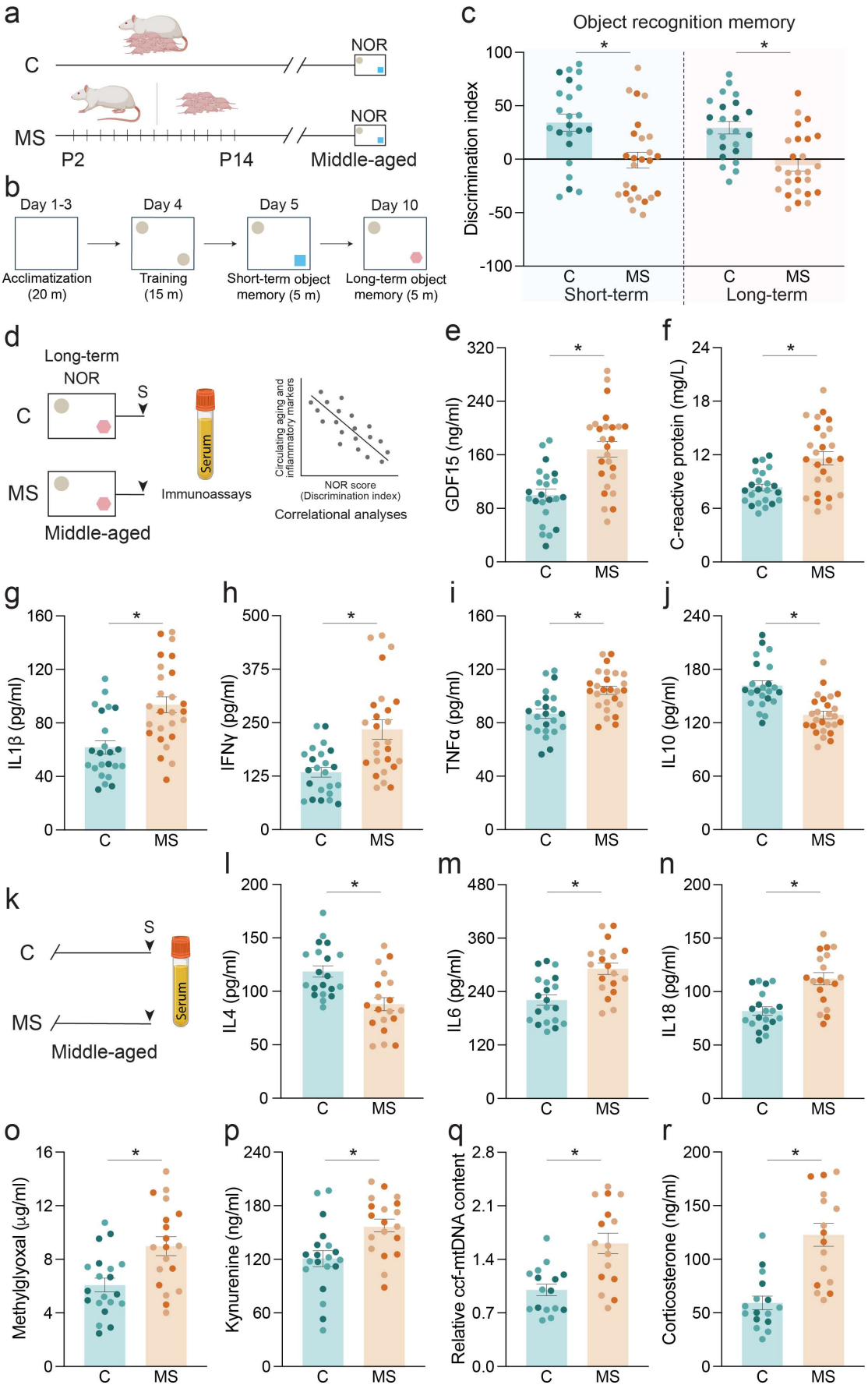
a
C
NOR
MS
NOR
P2
P14
Middle-aged
b
Day 1-3
Day 4
Day 5
Day 10
Acclimatization (20 m)
Training (15 m)
Short-term object memory (5 m)
Long-term object memory (5 m)
c
Object recognition memory
Discrimination index
Short-term
Long-term
d
Long-term NOR
C
MS
S
Serum
Immunoassays
Middle-aged
Circulating aging and inflammatory markers
NOR score (Discrimination index)
Correlational analyses
e
GDF15 (ng/ml)
f
C-reactive protein (mg/L)
g
IL1β (pg/ml)
h
IFNγ (pg/ml)
i
TNFα (pg/ml)
j
IL10 (pg/ml)
k
C
MS
S
Serum
Middle-aged
l
IL4 (pg/ml)
m
IL6 (pg/ml)
n
IL18 (pg/ml)
o
Methylglyoxal (μg/ml)
p
Kynurenine (ng/ml)
q
Relative ccf-mtDNA content
r
Corticosterone (ng/ml)

Fig. 1: A history of early-life stress impairs object recognition memory and drives peripheral inflammatory changes in middle-aged life.

a, Sprague-Dawley (SD) rats were subjected to early adversity using the maternal separation (MS) paradigm, which involved a daily separation (3 hours) of the litters from their dams from postnatal day 2 (P2) to P14, whilst control (C) litters were left undisturbed. **b,** Animals were tested for object recognition memory using the novel object recognition (NOR) task, wherein C and MS animals in middle-aged life (13-15 months) were first habituated to the NOR arena for 3 consecutive days prior to exposure on day 4 to two identical objects. Short and long-term object recognition memory were assessed on day 5 and day 10 respectively, by replacing one of the identical objects with a novel object of similar dimensions. **c,** Short and long-term object recognition memory were assessed by determining the discrimination index in middle-aged C and MS rats. Results are combined for both males (lighter shade) and females (darker shade), as no sex differences were noted in object recognition memory across both groups (C: n = 23 [14 males; 9 females], MS: 26 [14 males; 12 females]. **d,** Shown is a schematic representation of long-term NOR task in middle-aged C and MS animals, with serum harvested post-NOR task for analysis of inflammation, and aging-associated markers using immunoassays. The data was used to perform a correlational analyses between NOR task and inflammation associated markers. Shown are graphs for the following serum markers in middle-aged C and MS rats, namely **(e)** GDF15, **(f)** CRP, **(g)** IL1ß, **(h)** IFNγ, **(i)** TNFα, and **(j)** IL10, from the same cohort of C and MS animals [C: n = 23 (14 males; 9 females), MS: n = 26 (14 males; 12 females)]. **k,** Shown is a schematic representation of serum harvested from an independent cohort of middle-aged C and MS rats, which were not subjected to NOR task, for analysis of inflammation, aging, and stress-associated markers using immunoassay, assessment of circulating cell free mtDNA (ccf-mtDNA) content using the MitoQuicLy method. **l-p,** Shown are graphs for additional serum markers, namely **(l)** IL4, **(m)** IL6, **(n)** IL18, **(o)** methylglyoxal and **(p)** kynurenine, [C: n = 20 (10 males; 10 females), MS: n = 19 (10 males; 9 females]. **q-r,** Shown are graphs for **(q)** circulating cell-free mitochondrial DNA (ccf-mtDNA), **(r)** corticosterone levels using serum samples harvested from middle-aged C and MS rats (C: n = 16 (10 males; 6 females), MS: n = 16 (10 males; 6 females). Data are represented as mean ± SEM and with individual data points depicted as dots in the graphs (males – lighter shade; females – darker shade). *$p < 0.05$ as compared to C; unpaired Student's *t*-test.

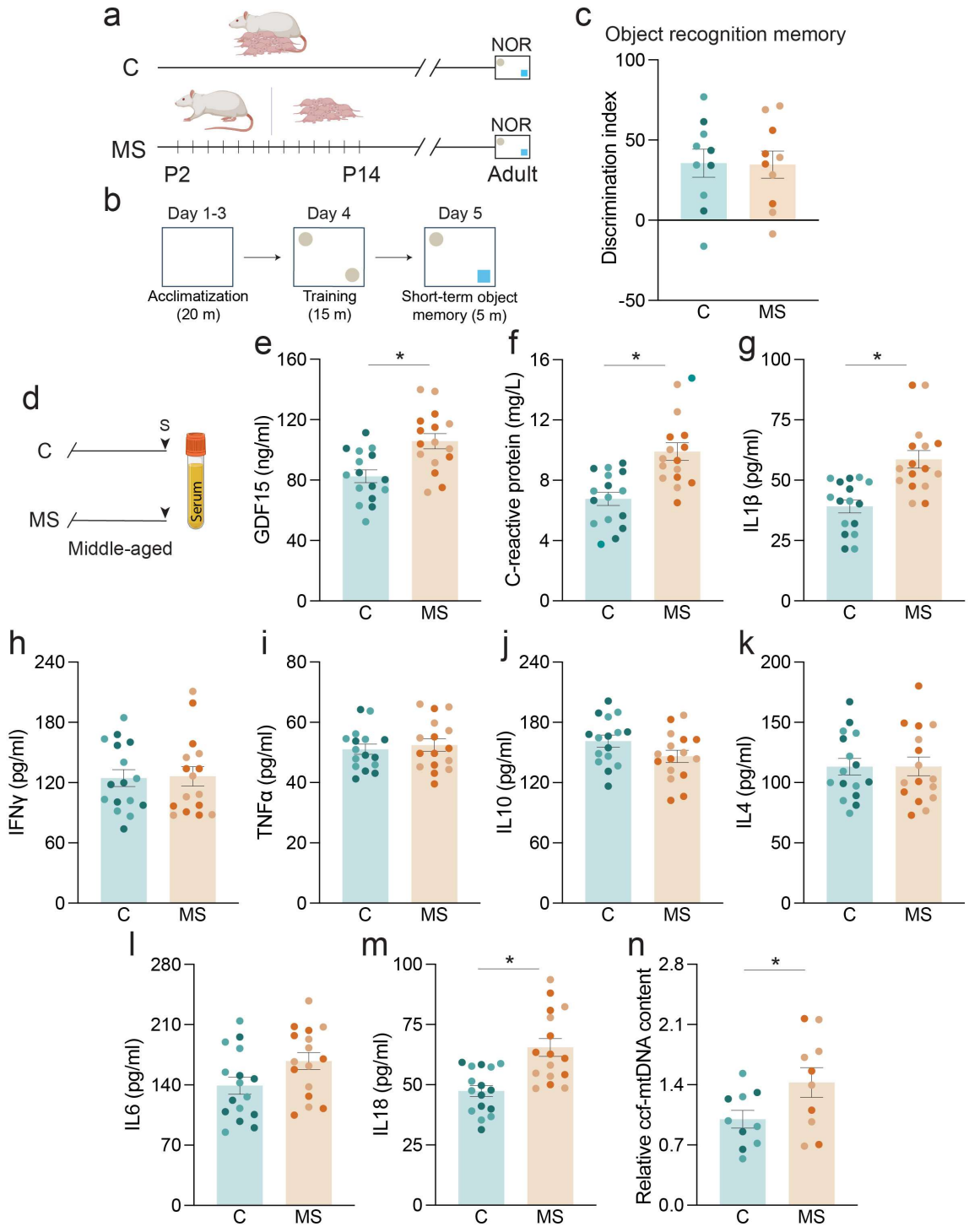

Extended data 1: Impact of a history of early-life stress on object recognition memory and peripheral inflammatory signatures in mature adulthood.

a, Shown is a schematic representation of the MS paradigm performed in SD rats. **b,** Animals were tested for object recognition memory using the novel object recognition (NOR) task, wherein C and MS animals in mature adulthood (6-7 months) were first habituated to the NOR arena for 3 consecutive days prior to exposure on day 4 to two identical objects. Short-term object recognition memory was assessed on day 5 by replacing one of the identical objects with a novel object of similar dimensions. **c,** Short-term object recognition memory was assessed

by determining the discrimination index in mature adult C and MS rats. Results are combined for both males (lighter shade) and females (darker shade) (C: n = 10 [6 males; 4 females], MS: 10 [6 males; 4 females]. **d,** Shown is a schematic representation of serum harvested from an independent cohort of mature adult C and MS rats for analysis of inflammation, aging-associated markers using immunoassay, as well as assessment of circulating cell free mtDNA (ccf-mtDNA) content using the MitoQuicLy method. Shown are graphs for the following serum markers in mature adult C and MS rats, namely **(e)** GDF15, **(f)** CRP, **(g)** IL1ß, **(h)** IFNγ, **(i)** TNFα, and **(j)** IL10, **(k)** IL4, **(l)** IL6, and **(m)** IL18 [C: n = 16 (8 males; 8 females), MS: n = 16 (8 males; 8 females)]. **n,** Shown is a graph for ccf-mtDNA using serum samples harvested from mature adult C and MS rats (C: n = 10 (6 males; 4 females), MS: n = 10 (6 males; 4 females). Data are represented as mean ± SEM and with individual data points depicted as dots in the graphs (males – lighter shade; females – darker shade). *$p < 0.05$ as compared to C; unpaired Student's *t*-test.

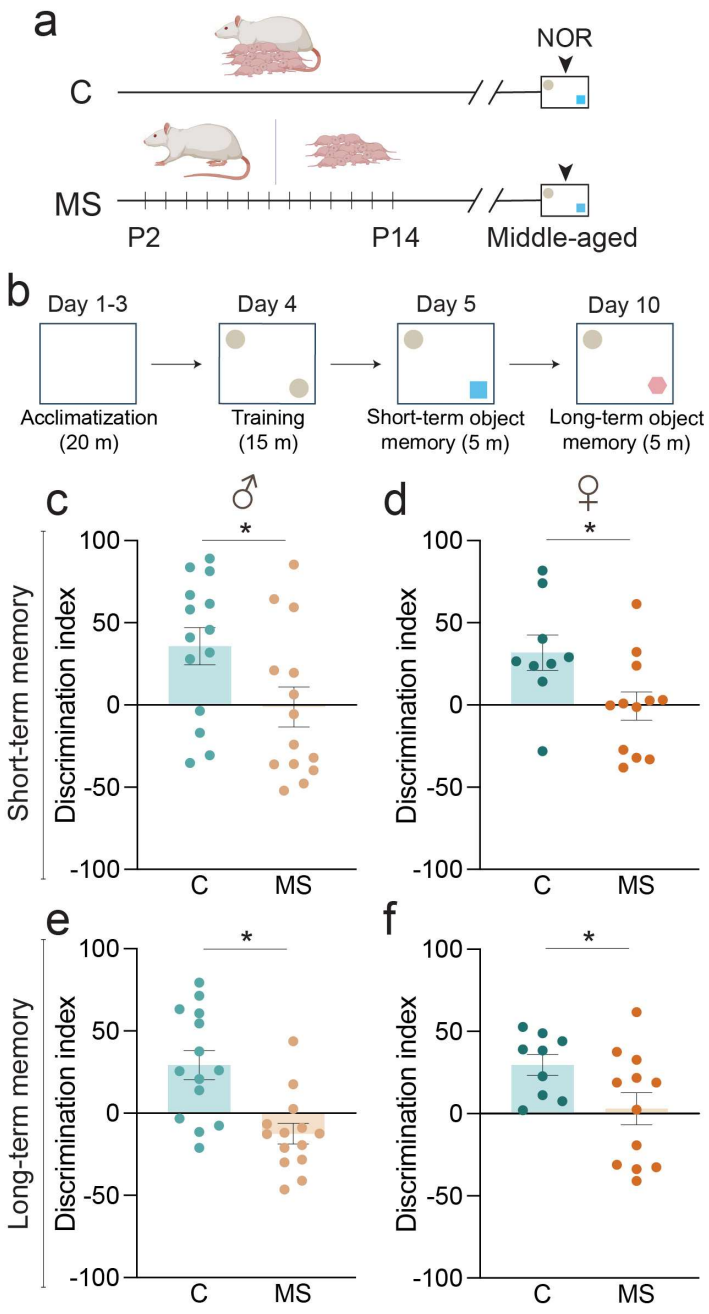

Extended data 2: A history of early-life stress impairs short and long-term object recognition memory in middle-aged male and female animals.

a, SD rats were subjected to early adversity using the maternal separation (MS) paradigm, which involved a daily separation (3 hours) of the litters from their dams from postnatal day 2 (P2) to P14, whilst control (C) litters were left undisturbed. **b,** Male and female animals from C and MS groups were tested for object recognition memory using NOR task, wherein middle-aged animals (13-15 months) were first habituated to the NOR arena for 3 consecutive days prior to exposure on day 4 to two identical objects. Short and long-term object recognition memory were assessed on day 5 and day 10 respectively, by replacing one of the identical objects with a novel object of similar dimensions. **c-f,** Graphs show short **(c-d)** and long-term **(e-f)** object recognition memory represented by determining the discrimination index in

middle-aged male **(c, e)** and female **(d, f)** rats from C and MS groups. (C: n = 14 males; 9 females, MS: 14 males; 12 females). Data are represented as mean ± SEM and with individual data points depicted as dots in the graphs. *$p < 0.05$ as compared to C; unpaired Student's *t*-test.

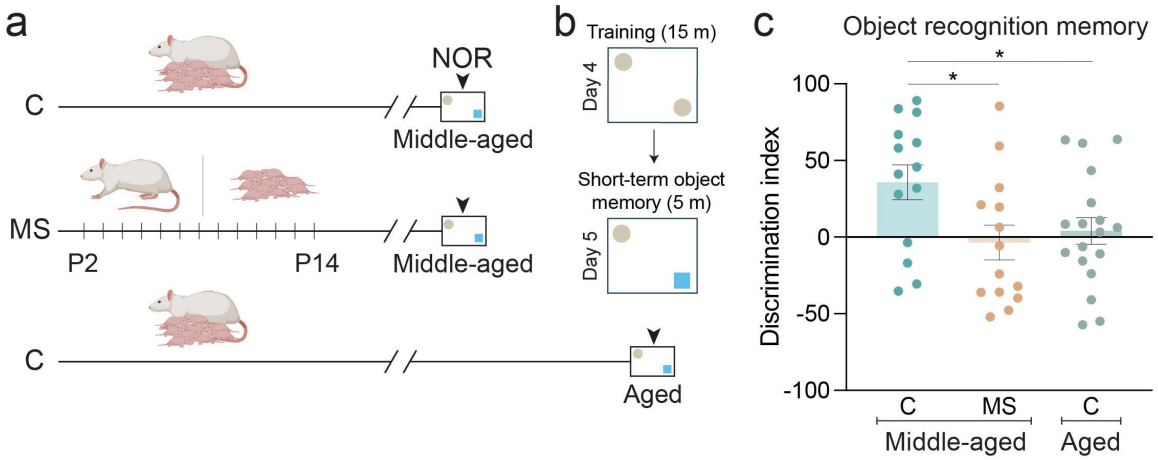

Extended data 3: Object recognition memory impairment observed in middle-aged MS rats is comparable to aged control animals.

a, Shown is a schematic representation of the MS paradigm performed in SD rats. **b,** Animals from C and MS groups were tested for object recognition memory using NOR task, wherein middle-aged C and MS (13-15 months) as well as aged C (22 months) animals were first habituated to the NOR arena for 3 consecutive days prior to exposure on day 4 to two identical objects. Short-term object recognition memory was assessed on day 5 replacing one of the identical objects with a novel object of similar dimensions. **c,** Short-term object recognition memory was assessed by determining the discrimination index in middle-aged C (n = 14 males), middle-aged MS (n = 14 males), and aged C animals (n = 18 males). Data are represented as mean ± SEM and with individual data points depicted as dots in the graphs. *$p < 0.05$ as compared to middle-aged C, one-way ANOVA followed by Tukey's post-hoc comparison.

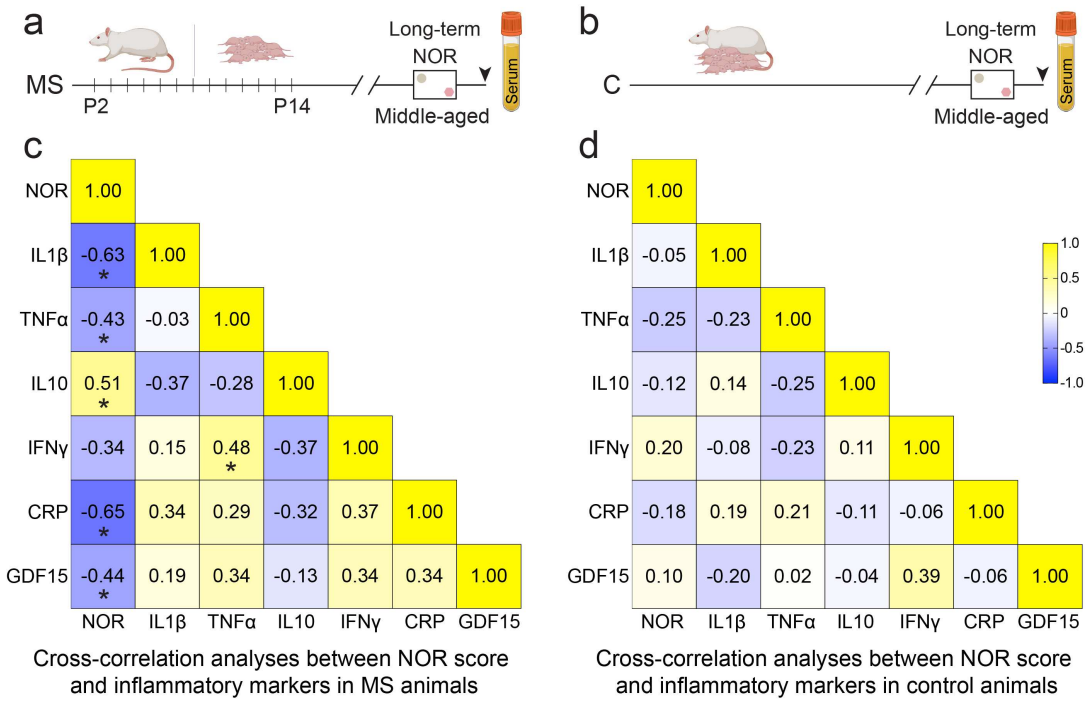

Extended data 4: Correlation matrix depicting an association between novel object recognition and inflammatory markers in middle-aged control and MS animals.

a-b, Shown is a schematic representation of the NOR task performed in **(a)** middle-aged MS and **(b)** C animals, with serum harvested post NOR task for analysis of inflammatory markers using immunoassays. **c-d,** Shown is a correlation matrix denoting Pearson's correlation coefficient (r) evaluated between discrimination index scored by novel object recognition (NOR) task and several circulating inflammatory markers namely IL1ß, TNFα, IL10, IFNγ, CRP, GDF15 in middle-aged **(c)** MS and **(d)** C animals (C: n = 23 [14 males; 9 females], MS: 26 [14 males; 12 females]). The underlying matrix indicates nature and extent of association, with positive correlation represented in yellow and negative correlation represented in blue. Data represented as a Pearson's correlation coefficient ranging from -1 to +1 and derived from a comparison to NOR score of +1. *$p < 0.05$; unpaired Student's *t*-test.

a

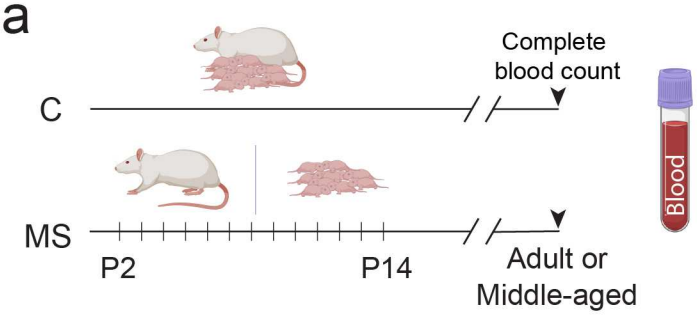

b

	C	MS	*p* value
WBC Count (/mm³)	3883 ± 468	5253 ± 434	$p = 0.057$
RBC Count (10^6/mm³)	7.82 ± 0.26	7.72 ± 0.32	$p = 0.809$
Platelet Count (/mm³)	706166 ± 42142	758333 ± 42306	$p = 0.130$
Haemoglobin (g/dL)	13.77 ± 0.36	13.05 ± 0.24	$p = 0.577$
Hematocrit (%)	41.02 ± 1.93	41.18 ± 2.40	$p = 0.959$

Adult

c

	C	MS	*p* value
WBC Count (/mm³)	3325 ± 537	6442 ± 914	$p = 0.015$*
RBC Count (10^6/mm³)	7.45 ± 0.36	8.10 ± 0.09	$p = 0.252$
Platelet Count (/mm³)	636333 ± 63827	998500 ± 33433	$p < 0.001$*
Haemoglobin (g/dL)	13.93 ± 0.71	14.35 ± 0.12	$p = 0.577$
Hematocrit (%)	42.20 ± 1.93	43.63 ± 0.25	$p = 0.478$

Middle-aged

Extended data 5: Impact of early-life stress on complete blood count measures in mature adult and middle-aged male animals.

a, Shown is a schematic representation of the MS paradigm performed in SD rats, with blood harvested from C and MS animals in mature adulthood or middle-aged life for assessment of complete blood count. **b-c,** Shown is a table for complete blood count measures namely white blood cells (WBCs), red blood cells (RBCs), platelets, haemoglobin, hematocrit in blood harvested from **(b)** adult and **(c)** middle-aged C and MS male animals (C: n = 6, MS: n = 6). Data are represented as mean ± SEM. *$p < 0.05$ as compared to C; unpaired Student's *t*-test.

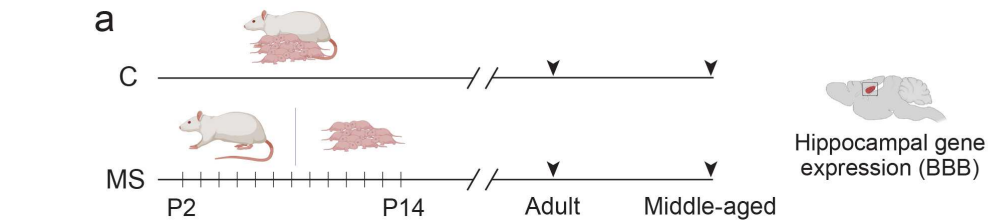

b

	Adult		
	C	MS	*p* value
Ntn1	1.00 ± 0.10	0.91 ± 0.07	*p* = 0.504
Mfsd2a	1.00 ± 0.10	0.89 ± 0.07	*p* = 0.391
Cldn5	1.00 ± 0.09	0.92 ± 0.05	*p* = 0.450
Cldn1	1.00 ± 0.19	0.86 ± 0.09	*p* = 0.517
Cldn3	1.00 ± 0.15	0.99 ± 0.11	*p* = 0.948
Cldn12	1.00 ± 0.11	0.95 ± 0.07	*p* = 0.696
Ocld	1.00 ± 0.12	0.90 ± 0.14	*p* = 0.611
Cd13	1.00 ± 0.13	1.06 ± 0.15	*p* = 0.769
Cd146	1.00 ± 0.06	0.93 ± 0.08	*p* = 0.509
Vcam1	1.00 ± 0.10	0.98 ± 0.06	*p* = 0.868
Pdgrfb	1.00 ± 0.12	0.97 ± 0.08	*p* = 0.856
Tjp1	1.00 ± 0.14	0.87 ± 0.05	*p* = 0.503
Tjp2	1.00 ± 0.12	0.90 ± 0.09	*p* = 0.828
Tjp3	1.00 ± 0.19	0.97 ± 0.10	*p* = 0.896
Aqp4	1.00 ± 0.07	0.97 ± 0.08	*p* = 0.794

c

	Middle-aged			
	C	MS	*p* value	FDR *p* value
Ntn1	1.00 ± 0.09	0.59 ± 0.05	*p* = 0.012 *	*p* = 0.054
Mfsd2a	1.00 ± 0.14	0.49 ± 0.05	*p* = 0.002 *	*p* = 0.032 *
Cldn5	1.00 ± 0.09	0.54 ± 0.05	*p* = 0.005 *	*p* = 0.038 *
Cldn1	1.00 ± 0.23	0.61 ± 0.05	*p* = 0.018 *	*p* = 0.055
Cldn3	1.00 ± 0.16	0.87 ± 0.05	*p* = 0.426	*p* = 0.506
Cldn12	1.00 ± 0.12	0.89 ± 0.05	*p* = 0.497	*p* = 0.506
Ocld	1.00 ± 0.11	0.65 ± 0.05	*p* = 0.035 *	*p* = 0.069
Cd13	1.00 ± 0.14	0.72 ± 0.05	*p* = 0.085	*p* = 0.128
Cd146	1.00 ± 0.14	0.60 ± 0.05	*p* = 0.015 *	*p* = 0.054
Vcam1	1.00 ± 0.11	1.12 ± 0.05	*p* = 0.475	*p* = 0.506
Pdgrfb	1.00 ± 0.16	0.68 ± 0.05	*p* = 0.053	*p* = 0.088
Tjp1	1.00 ± 0.13	0.80 ± 0.05	*p* = 0.224	*p* = 0.306
Tjp2	1.00 ± 0.12	0.89 ± 0.05	*p* = 0.506	*p* = 0.506
Tjp3	1.00 ± 0.16	0.66 ± 0.05	*p* = 0.037 *	*p* = 0.069
Aqp4	1.00 ± 0.07	0.65 ± 0.05	*p* = 0.033 *	*p* = 0.069

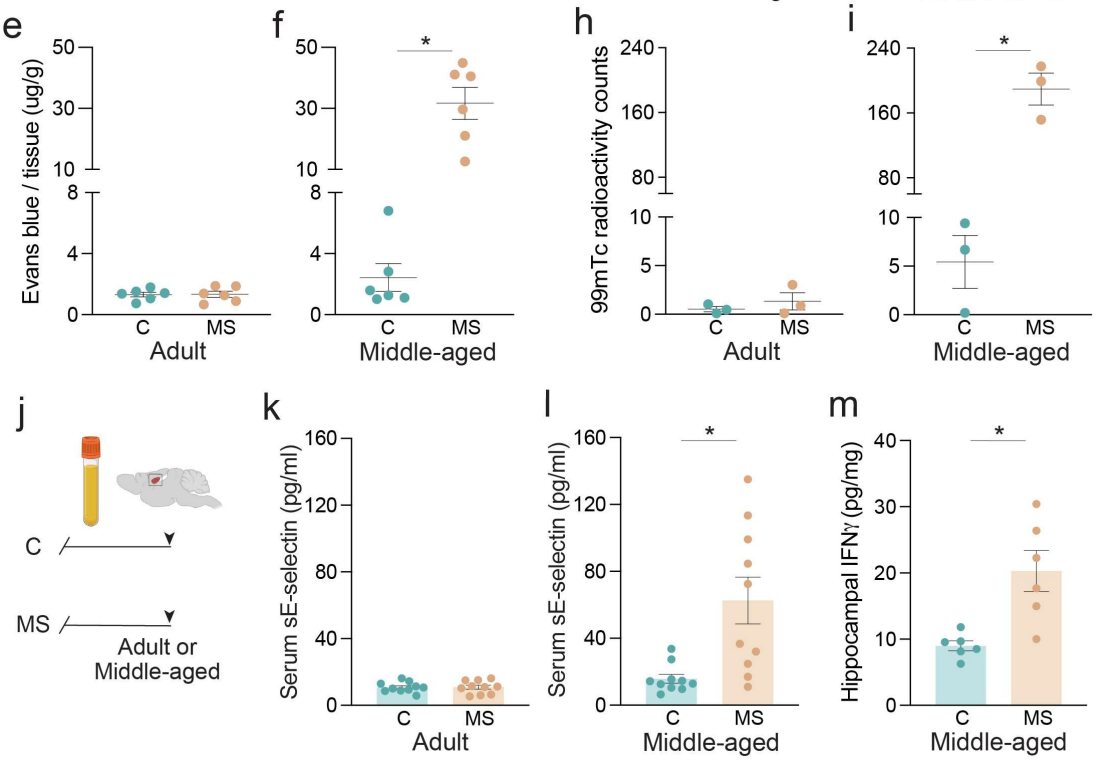

Fig. 2: Early-life stress alters the blood-brain barrier integrity in middle-aged animals.

a, Shown is a schematic representation of the maternal separation (MS) paradigm with blood-brain barrier (BBB) integrity assessed in mature adulthood (6-7 months) or middle-aged life (13-15 months), with integrity of the blood-brain barrier (BBB) was assessed using a hippocampal gene expression profiling, Evans blue (EB) extravasation assay, Technitium-99 (99mTc) radiotracer assay, serum soluble E-selectin (sE-selectin) concentrations and hippocampal IFNγ levels**. b-c,** Shown is the relative hippocampal gene expression in **(b)** mature adult and **(c)** middle-aged C and MS animals for genes associated with BBB formation, tight junctions and neurovasculature. The underlying heatmap indicates the nature and extent of regulation, with upregulated genes represented in red and downregulated genes represented in blue. Data are represented as a fold change of age-matched C rats (mean ± SEM) with gene expression normalized to 18S rRNA (Adult- C: n = 10 males, MS: n = 11 males; Middle-aged- C: n = 9 males, MS: n = 11 males). **d,** Shown is a schematic representation of Evans blue extravasation assay to investigate BBB leakiness in adult or middle-aged C and MS animals. **e-f,** Graphical representation of Evans blue extravasation into hippocampal parenchyma in **(e)** mature adult and **(f)** middle-aged rats (C: n = 6 males, MS: n = 6 males). **g,** Shown is a schematic representation of Technitium-99 (99mTc) radiotracer paradigm followed by *ex vivo* SPECT (Single Photon Emission Computed Tomography) to determine BBB integrity in adult or middle-aged C and MS rats. **h-i,** Graph indicates 99mTc radioactivity counts in brain parenchyma derived post *ex vivo* SPECT scan of **(h)** mature adult and **(i)** middle-aged C and MS rat brains (C: n = 3 males, MS: n = 3 males). **j,** Shown is a schematic representation of the maternal separation (MS) paradigm with integrity of the BBB was assessed using serum soluble E-selectin (sE-selectin) concentrations and hippocampal IFNγ levels in mature adulthood or middle-aged life. **k-l,** Shown is a graph for soluble E-selectin (sE-selectin) levels in serum harvested from **(k)** adult and **(l)** middle-aged C and MS rats (C: n = 10 males, MS: n = 10 males). **m,** Graph indicates hippocampal IFNγ levels assessed using ELISA in middle-aged C and MS rats (C: n = 6 males, MS: n = 6 males). Data are represented as mean ± SEM, with individual data points depicted as dots in the graphs. $*p < 0.05$ as compared to C; unpaired Student's *t*-test. For gene expression data, false discovery rate (FDR) corrected *p*-values were also determined using the Benjamini-Hochberg method.

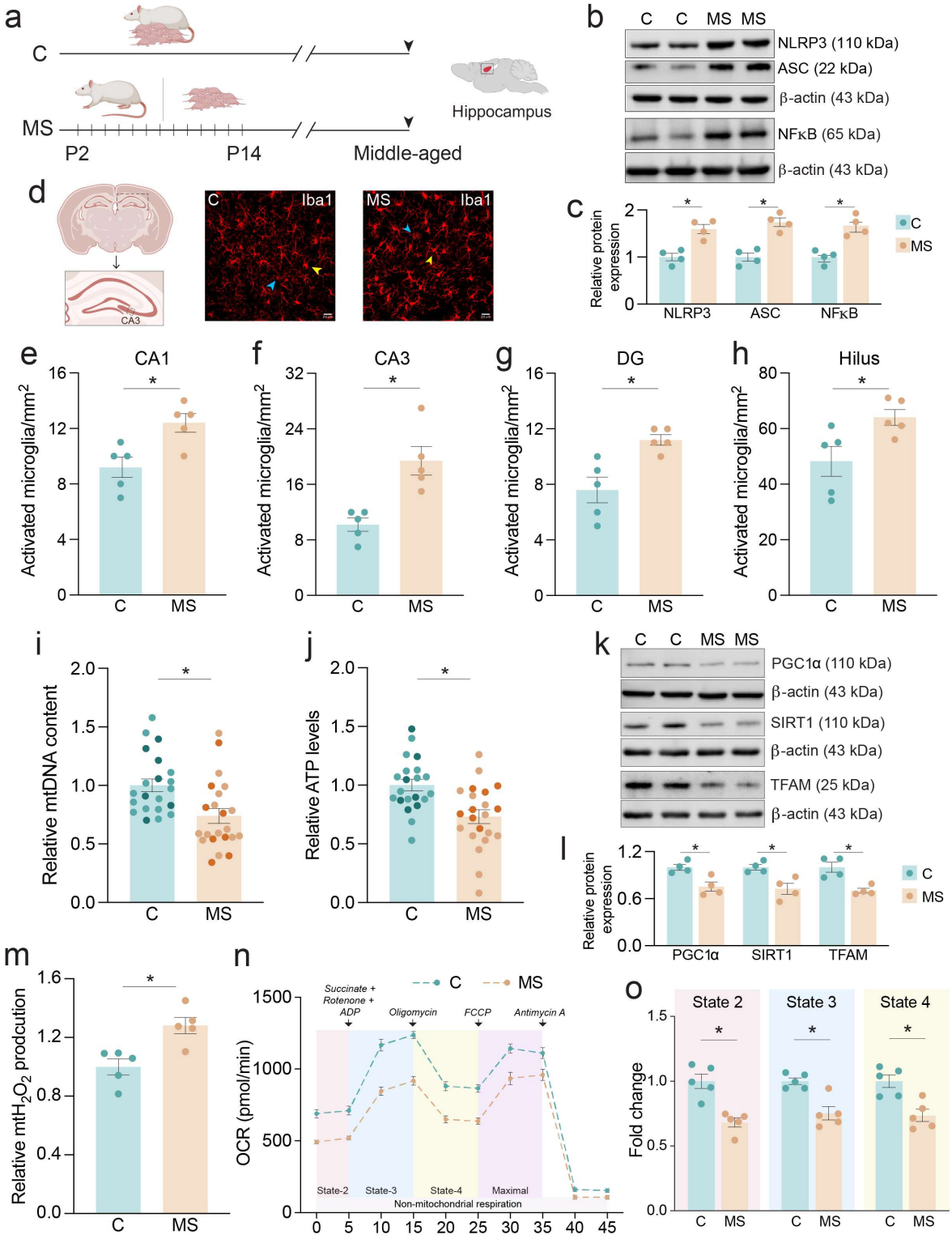

Fig. 3: Early-life stress drives neuroinflammatory signatures and disrupts mitochondrial status in the hippocampi of middle-aged animals.

a, Shown is a schematic representation of the maternal separation (MS) paradigm followed by assessing neuroinflammation-associated signatures in the hippocampus in middle-aged life, namely NLRP3 inflammasome marker expression, and immunofluorescence studies to assess activation of microglia using Iba1. **b,** Shown are representative western blots for hippocampal protein expression of NLRP3, ASC, and NF-κB in middle-aged C and MS rats, along with β-

actin used as a protein loading control. **c,** Graph depicts relative protein expression for NLRP3 inflammasome markers namely NLRP3, ASC, and NF-κB in the hippocampi of middle-aged C and MS rats. Data is represented as a fold change of middle-aged C rats (mean ± SEM) with protein expression normalized to β-actin (C: n = 4 males, MS: n = 4 males). **d,** Shown is a representative Iba1-immunostained hippocampal section through the CA3 hippocampal subfield from middle-aged C and MS rat, where microglial morphology associated with activation denoted by yellow arrowhead and a resting state microglia indicated by blue arrowhead, scale: 20 μm. **e-h,** Graphs represent the number of activated microglia/mm^2 in the hippocampal subfields namely **(e)** CA1, **(f)** CA3, **(g)** DG, and **(h)** hilus from middle-aged C and MS rats (C: n = 5 males, MS: n = 5 males). **i-j,** Graphs represent relative (**i)** mtDNA content and **(j)** cellular ATP levels assessed in hippocampi derived from middle-aged C and MS male and female animals (C: n = 21 [14 males; 7 females], MS: n = 22 [14 males; 8 females]). **k,** Shown are representative western blots for hippocampal protein expression of modulators of mitochondrial biogenesis, namely PGC-1α, SIRT1, and TFAM in the hippocampi of middle-aged C and MS rats, along with β-actin used as a protein loading control. **l,** Graphs depicts relative protein expression for PGC-1α, SIRT1, and TFAM in the hippocampi of middle-aged C and MS rats. Data is represented as a fold change of middle-aged C rats (mean ± SEM) with protein expression normalized to β-actin (C: n = 4 males, MS: n = 4 males). **m**, Graph represents mitochondrial reactive oxygen species (mtROS) production in the form of hydrogen peroxide in mitochondria (mtH_2O_2) harvested from hippocampi of middle-aged C and MS rats (C: n = 5 males, MS: n = 5 males). **n,** Shown is a seahorse plot for isolated mitochondria (20 μg) derived from the hippocampi of middle-aged C and MS rats, with measurements for complex-I dependent state-2 respiration in limiting endogenous ADP and succinate, complex-II dependent state-3 respiration post-injection of rotenone + Succinate + ADP, and oligomycin (2μM) induced state-4 respiration (C: n = 5 males, MS: n = 5 males). **o,** Graph depicts relative state-2, state-3, state-4 respiration evaluated by seahorse analysis (C: n = 5 males, MS: n = 5 males). Data are represented as mean ± SEM, with individual data points depicted as dots in the graphs (males – lighter shade; females – darker shade). *$p < 0.05$ as compared to C; unpaired Student's *t*-test.

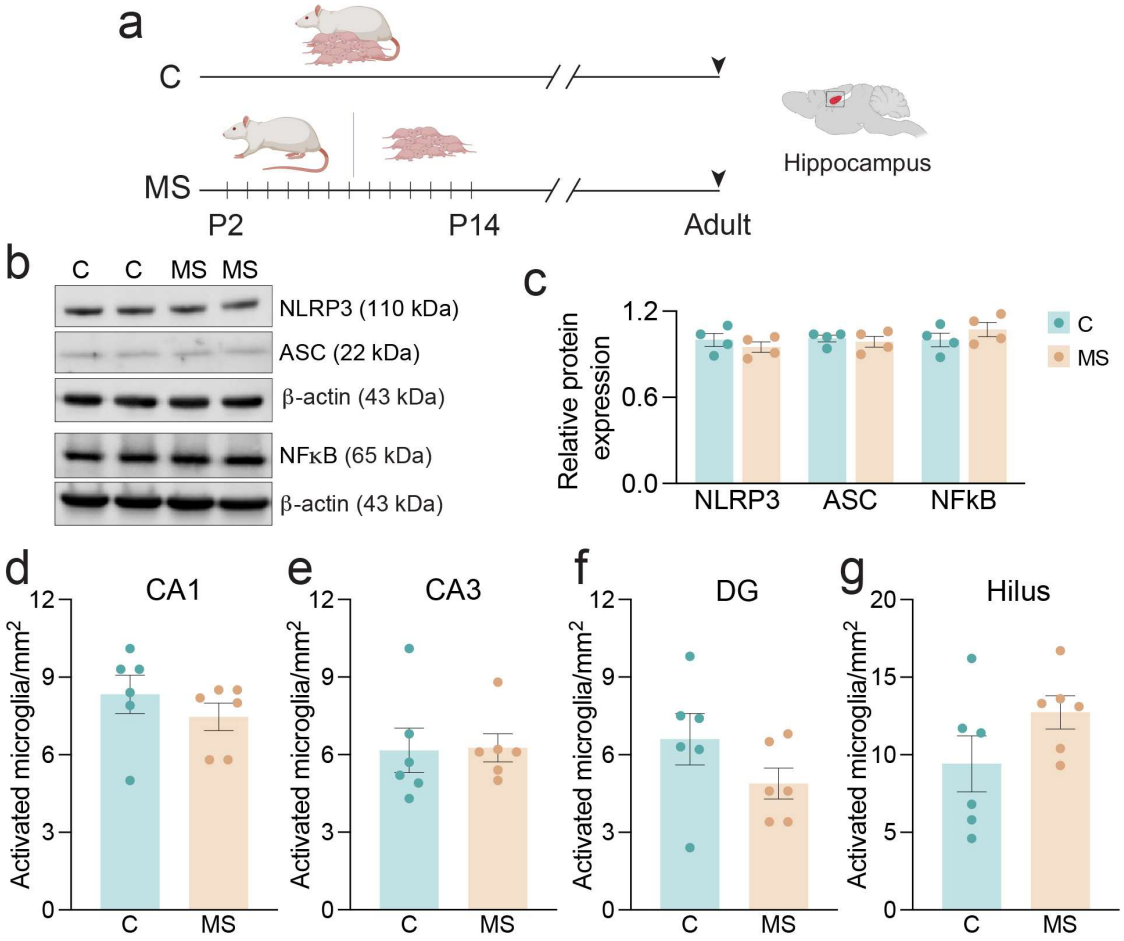

Extended data 6: Early-life stress does not alter neuroinflammatory signatures in the hippocampi of mature adult animals.

a, Shown is a schematic representation of the maternal separation (MS) paradigm followed by assessing neuroinflammation-associated signatures in the hippocampus in mature adulthood, namely NLRP3 inflammasome marker expression, and immunofluorescence studies to assess activation of microglia using Iba1. **b,** Shown are representative western blots for hippocampal protein expression of NLRP3, ASC, and NF-κB in mature adult C and MS rats, along with β-actin used as a protein loading control. **c,** Graph depicts relative protein expression for NLRP3 inflammasome markers namely NLRP3, ASC, and NF-κB in the hippocampi of adult C and MS rats. Data is represented as a fold change of middle-aged C rats (mean ± SEM) with protein expression normalized to β-actin (C: n = 4 males, MS: n = 4 males). **d-g,** Graphs represent the number of activated microglia/mm^2 in the hippocampal subfields namely **(d)** CA1, **(e)** CA3, **(f)** DG, and **(g)** hilus from adult C and MS rats (C: n = 6 males, MS: n = 6 males). Data are represented as mean ± SEM, with individual data points depicted as dots in the graphs. *p < 0.05 as compared to C; unpaired Student's t-test.

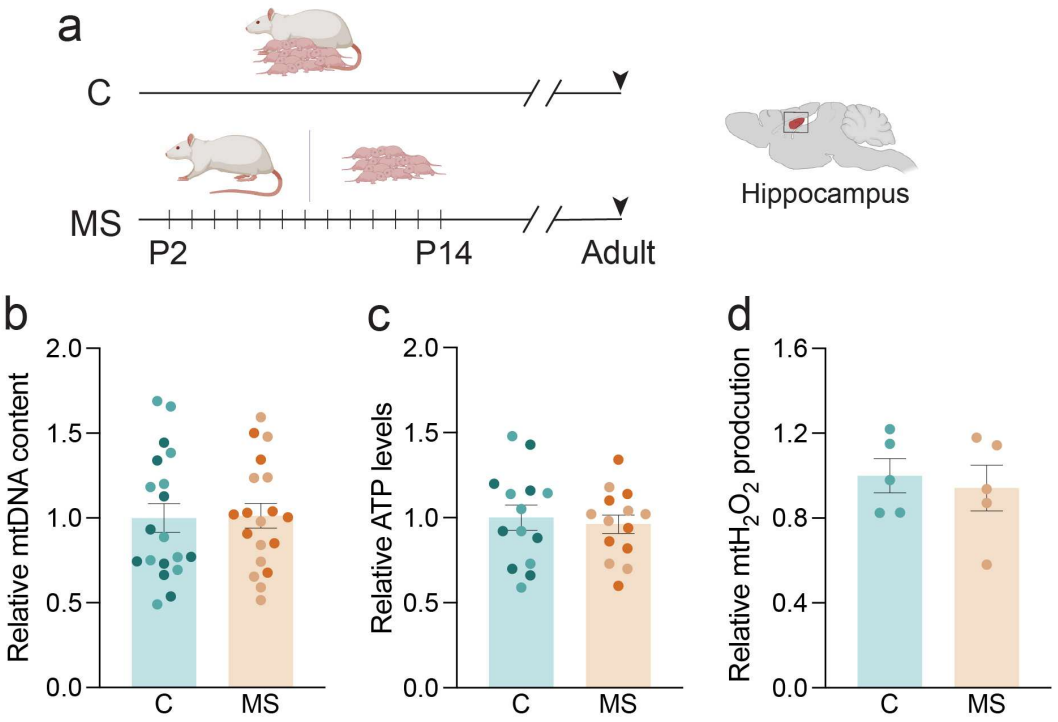

Extended data 7: Early-life stress does not disrupt mitochondrial health and function in the hippocampi of mature adult animals.

a, Shown is a schematic representation of the maternal separation (MS) paradigm followed by assessing mtDNA content, cellular ATP levels and mtROS production in hippocampi of adult C and MS animals. **b,** Graphs represent relative mtDNA content in hippocampi derived from adult C and MS male and female animals (C: n = 19 [10 males; 9 females], MS: n = 19 [10 males; 9 females]). **c,** graphical representation of relative cellular ATP levels assessed in hippocampi derived from mature adult C and MS male and female animals (C: n = 14 [7 males; 7 females], MS: n = 14 [7 males; 7 females]). **d**, Graph represents mitochondrial reactive oxygen species (mtROS) production in the form of hydrogen peroxide in mitochondria (mtH_2O_2) harvested from hippocampi of mature adult C and MS rats (C: n = 5 males, MS: n = 5 males). Data are represented as mean ± SEM, with individual data points depicted as dots in the graphs (males – lighter shade; females – darker shade). *$p < 0.05$ as compared to C; unpaired Student's *t*-test.

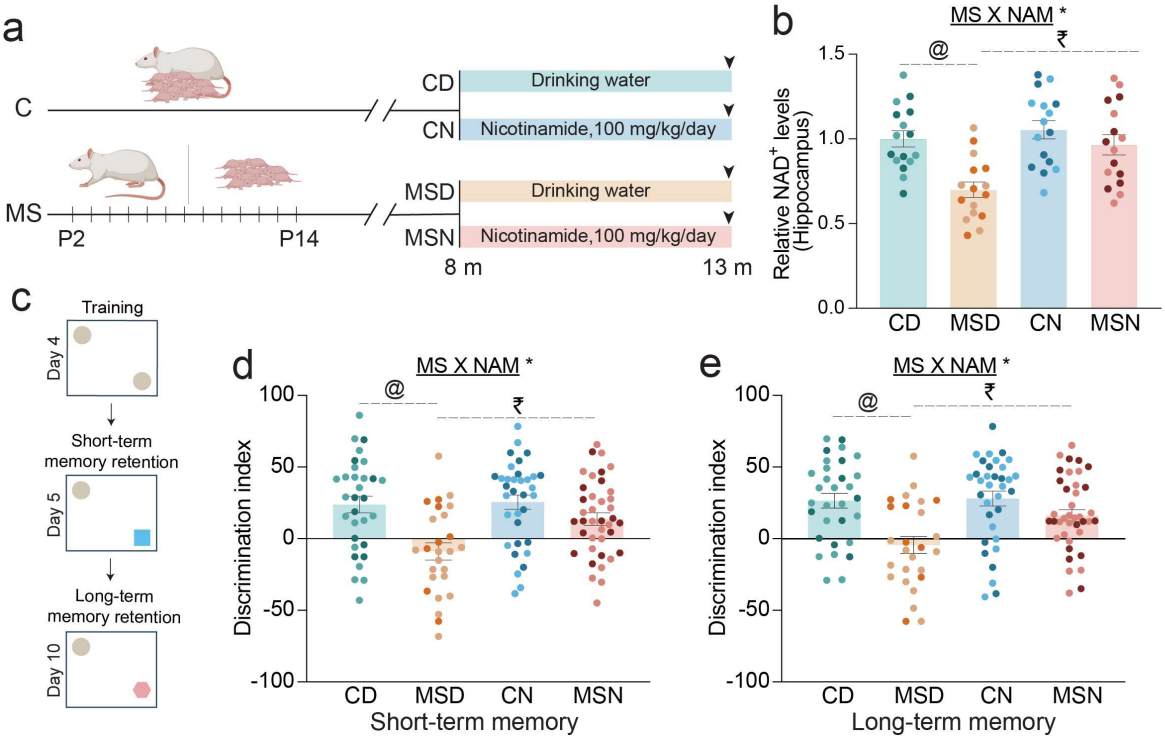

Fig. 4: Nicotinamide supplementation attenuates the impact of early-life stress on object recognition memory in middle-aged life.

a, Shown is a schematic representation of the paradigm for nicotinamide (NAM; 100 mg/kg/day) supplementation through drinking water commencing from 8 months of age for 5 months (CD and MSD: age-matched C and MS animals with regular drinking water; CN and MSN: age-matched C and MS animals with NAM supplemented drinking water). **b,** Graph depicts relative nicotinamide adenine dinucleotide (NAD^+) levels evaluated in the hippocampi of middle-aged CD, MSD, CN and MSN rats (n= 16 [8 males; 8 females] per group). **c,** Animals were tested for object recognition memory using the NOR task, wherein 13-month old CD, MSD, CN and MSN animals were first habituated to the NOR arena prior to testing short and long-term object recognition memory on day 5 and day 10 respectively, by replacing one of the identical objects with a novel object of similar dimensions. **d-e,** Graphs indicate discrimination index for **(d)** short and **(e)** long-term object recognition memory in middle-aged CD, MSD, CN and MSN rats. Results are combined for both males and females (CD: n = 31 [21 males; 10 females], MSD: n = 26 [18 males; 8 females], CN: n = 34 [19 males; 15 females], MSN: n = 39 [23 males; 16 females]. Data are represented as mean ± SEM with individual data points depicted as dots in the graphs (males – lighter shade; females – darker shade). $^{*}p < 0.05$ (Interaction effect on Two-way ANOVA between the variables of MS and NAM); $^{@}p < 0.05$ (compared with CD: Control group on regular drinking water, Tukey's post-hoc test); $^{₹}p < 0.05$ (compared with MSD: MS group on regular drinking water, Tukey's post-hoc test).

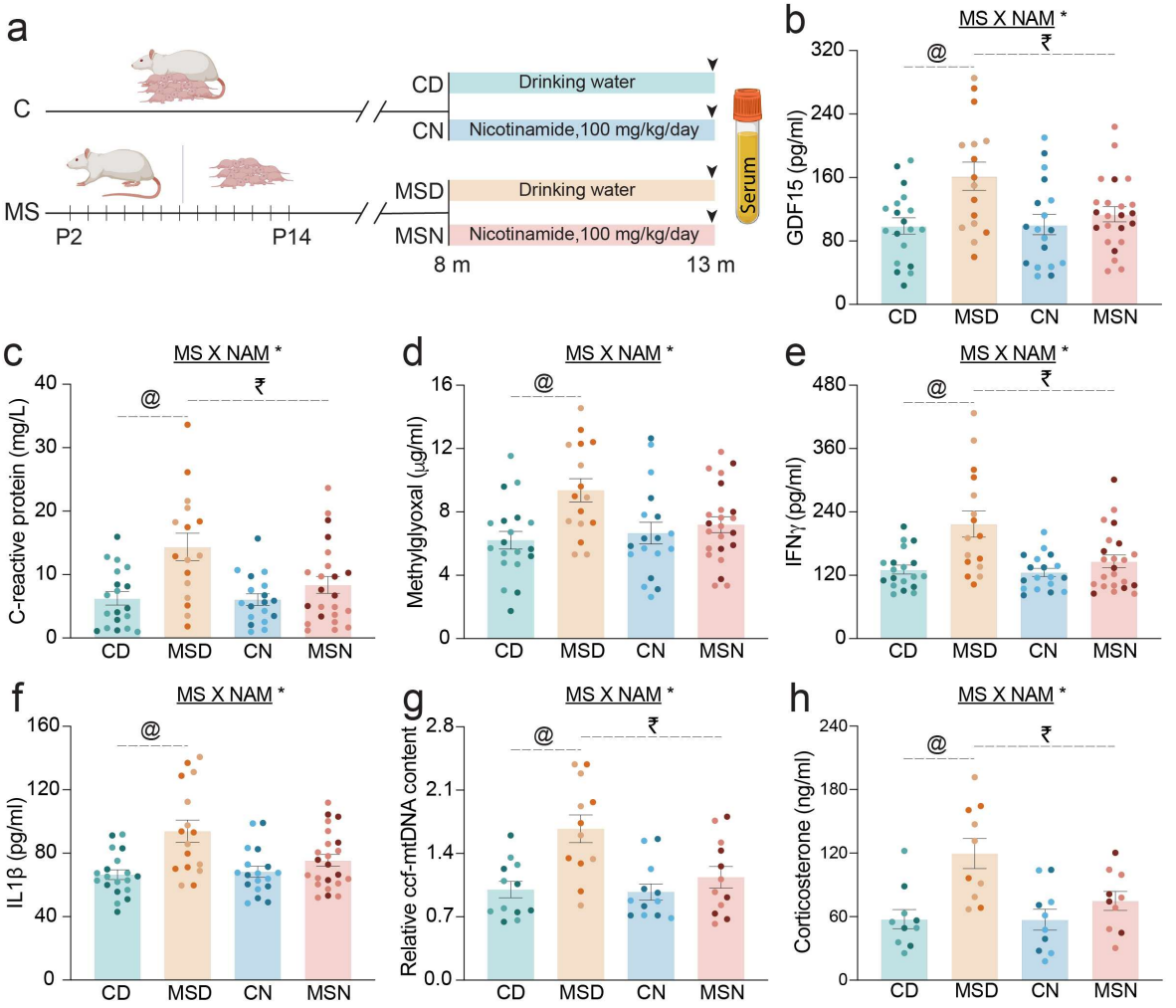

i

	CD	MSD	CN	MSN	Interaction MS X NAM
WBC count (/mm³)	3657 ± 409	6600 ± 714@	3830 ± 436	3978 ± 447₹	F (1, 24) = 7.315 p = 0.012 *
RBC count (/mm³)	7.68 ± 0.30	8.06 ± 0.08	7.56 ± 0.30	8.12 ± 0.12	F (1, 24) = 0.164 p = 0.689
Platelet count (/mm³)	616857 ± 68800	1018142 ± 39502@	678857 ± 86041	774571 ± 59195	F (1, 24) = 5.428 p = 0.029 *
Haemoglobin (g/dL)	13.88 ± 0.60	14.47 ± 0.16	14.00 ± 0.46	14.63 ± 0.13	F (1, 24) = 0.003 p = 0.957
Hematocrit (%)	42.26 ± 1.63	44.09 ± 0.50	42.18 ± 1.43	44.51 ± 0.46	F (1, 24) = 0.048 p = 0.828

Fig. 5: Nicotinamide supplementation attenuates the impact of early-life stress on peripheral inflammation in middle-aged life.

a, Shown is a schematic representation of the paradigm for nicotinamide (NAM; 100 mg/kg/day) supplementation through drinking water commencing from 8 months of age for 5 months (CD and MSD: age-matched C and MS animals with regular drinking water; CN and MSN: age-matched C and MS animals with NAM supplemented drinking water). **f,** Schematic representation showing serum harvested from middle-aged CD, MSD, CN and MSN animals, which was used for analysis of inflammation, aging and stress-associated markers using ELISA and to evaluate circulating cell free mtDNA (ccf-mtDNA) content using the MitoQuicLy

method. **b-f,** Shown are graphs for serum markers namely **(b)** GDF15, **(c)** CRP, **(d)** methylglyoxal, **(e)** IFNγ, and **(f)** IL1ß (CD: n = 19 [11 males; 8 females], MSD: n = 16 [8 males; 8 females], CN: n = 18 [10 males; 8 females], MSN: n = 23 [15 males; 8 females]). **g,** Graph depicts relative ccf-mtDNA levels in serum harvested from middle-aged CD, MSD, CN and MSN animals (n = 12 [6 males and 6 females] per group). **h,** Shown is a graph for circulating corticosterone levels in middle-aged CD, MSD, CN and MSN animals (n = 10 [6 males and 4 females] per group). **i,** Shown is a table for complete blood count measures namely white blood cells (WBCs) red blood cells (RBCs), platelets, haemoglobin, hematocrit in blood harvested from middle-aged CD, MSD, CN and MSN animals (n = 7 males per group). Data are the mean ± SEM with individual data points depicted as dots in the graphs (males – lighter shade; females – darker shade). $^{*}p < 0.05$ (Interaction effect on Two-way ANOVA between the variables of MS and NAM); $^{@}p < 0.05$ (compared with CD: Control group on regular drinking water, Tukey's post-hoc test); $^{₹}p < 0.05$ (compared with MSD: MS group on regular drinking water, Tukey's post-hoc test).

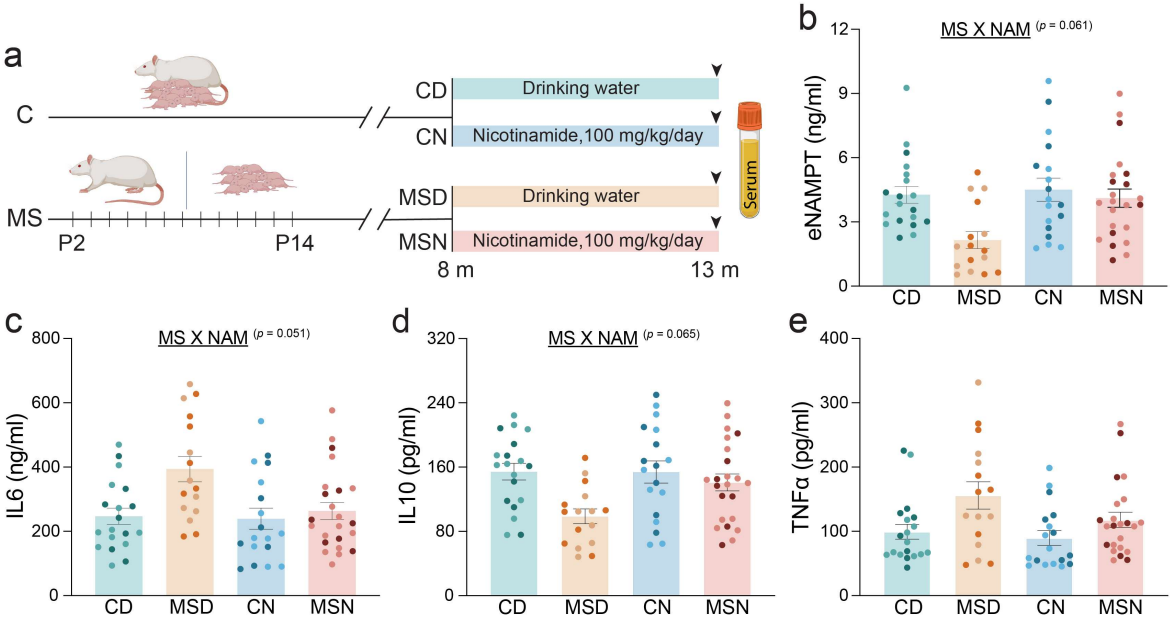

Extended data 8: Impact of nicotinamide supplementation on peripheral inflammatory markers in middle-aged rats with a history of early-life stress.

a, Shown is a schematic representation of the paradigm for nicotinamide (NAM; 100 mg/kg/day) supplementation through drinking water commencing from 8 months of age for 5 months (CD and MSD: age-matched C and MS animals with regular drinking water; CN and MSN: age-matched C and MS animals with NAM supplemented drinking water). Serum was harvested for analysis of inflammation-associated markers using immunoassays. **b-e**, Shown are graphs for serum markers namely **(b)** eNAMPT, **(c)** IL6, **(d)** IL10, and **(e)** TNFα levels in middle-aged CD, MSD, CN and MSN male and female animals (CD: n = 19 [11 males; 8 females], MSD: n = 16 [8 males; 8 females], CN: n = 18 [10 males; 8 females], MSN: n = 23 [15 males; 8 females]). Data are the mean ± SEM with individual data points depicted as dots in the graphs (males – lighter shade; females – darker shade). $^{*}p < 0.05$ (Interaction effect on

Two-way ANOVA between the variables of MS and NAM); $^{@}p < 0.05$ (compared with CD: Control group on regular drinking water, Tukey's post-hoc test); $^{₹}p < 0.05$ (compared with MSD: MS group on regular drinking water, Tukey's post-hoc test).

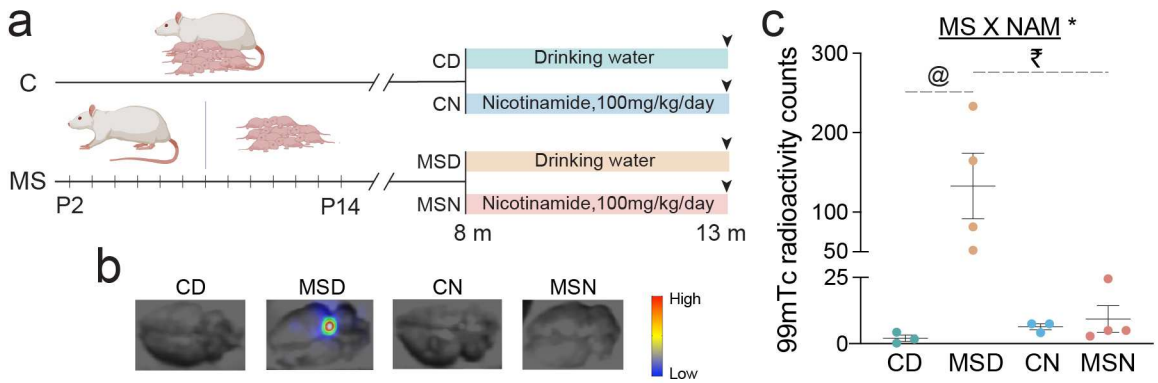

d

Hippocampal gene expression (BBB)	CD	MSD	CN	MSN	Interaction MS X NAM
Ntn1	1.00 ± 0.09	0.63 ± 0.07 @	1.01 ± 0.12	0.96 ± 0.09 ₹	F (1, 36) = 4.217 *p* = 0.047 *
Mfsd2a	1.00 ± 0.07	0.64 ± 0.09 @	0.95 ± 0.07	0.93 ± 0.09	F (1, 36) = 4.129 *p* = 0.049 *
Cldn5	1.00 ± 0.14	0.72 ± 0.07	1.02 ± 0.10	0.96 ± 0.13	F (1, 36) = 2.173 *p* = 0.149
Cldn1	1.00 ± 0.15	0.77 ± 0.17	1.07 ± 0.14	0.91 ± 0.15	F (1, 36) = 0.055 *p* = 0.815
Cldn3	1.00 ± 0.20	0.78 ± 0.08	0.87 ± 0.08	0.79 ± 0.13	F (1, 36) = 0.285 *p* = 0.596
Cldn12	1.00 ± 0.12	0.71 ± 0.07	1.07 ± 0.12	0.99 ± 0.12	F (1, 36) = 0.893 *p* = 0.351
Ocln	1.00 ± 0.08	0.61 ± 0.09 @	0.96 ± 0.08	0.93 ± 0.10	F (1, 36) = 2.807 *p* = 0.049 *
Cd13	1.00 ± 0.12	0.68 ± 0.09	1.02 ± 0.12	0.78 ± 0.14	F (1, 36) = 1.227 *p* = 0.728
Cd146	1.00 ± 0.08	0.60 ± 0.05	1.06 ± 0.11	0.91 ± 0.10	F (1, 36) = 1.746 *p* = 0.194
Vcam1	1.00 ± 0.14	1.06 ± 0.11	0.84 ± 0.08	0.80 ± 0.12	F (1, 36) = 1.972 *p* = 0.659
Pdgrfb	1.00 ± 0.12	0.69 ± 0.11	0.83 ± 0.11	0.75 ± 0.11	F (1, 36) = 9.767 *p* = 0.329
Aqp4	1.00 ± 0.09	0.57 ± 0.05 @	0.97 ± 0.10	0.89 ± 0.09	F (1, 36) = 4.187 *p* = 0.048 *

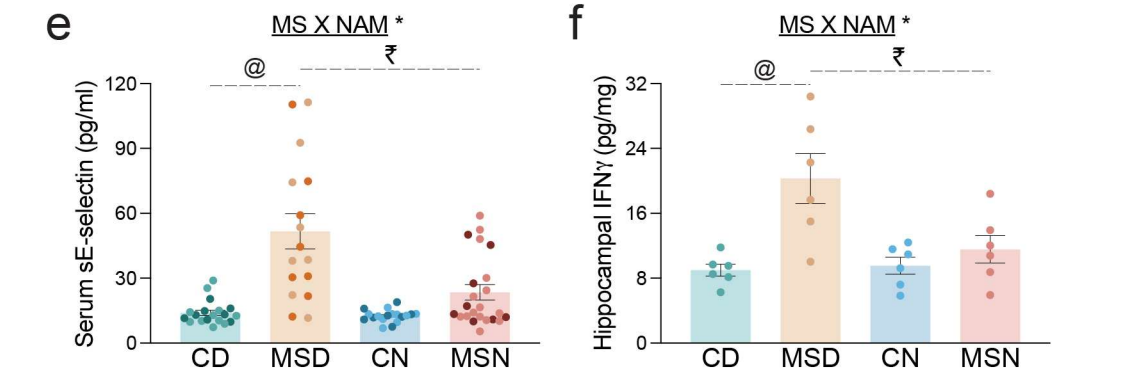

Fig. 6: Nicotinamide supplementation preserves blood brain barrier integrity in middle-aged rats with a history of early-life stress.

a, Shown is a schematic representation of the paradigm for nicotinamide (NAM; 100 mg/kg/day) supplementation through drinking water commencing from 8 months of age for 5

months (CD and MSD: age-matched C and MS animals with regular drinking water; CN and MSN: age-matched C and MS animals with NAM supplemented drinking water). **b-c,** Integrity of the blood brain barrier (BBB) was assessed using a Technitium-99 (99mTc) radiotracer assay in CD, MSD, CN and MSN animals in middle-aged life. **b,** Shown are representative *ex-vivo* SPECT images depicting 99mTc radioactivity in the brains of middle-aged CD, MSD, CN and MSN rats **c,** Graph depicts 99mTc radioactivity counts in the brain of middle-aged CD, MSD, CN and MSN rats (n = 3-4 males per group). **d,** Shown is the relative hippocampal gene expression in middle-aged CD, MSD, CN and MSN animals for genes associated with BBB formation, tight junctions and neurovasculature. The underlying heatmap indicates the nature and extent of regulation, with upregulated genes represented in red and downregulated genes represented in blue. Data are represented as a fold change of middle-aged CD rats (mean ± SEM) with gene expression normalized to 18S rRNA (n= 10 males per group). **e,** Shown is a graph for soluble E-selectin (sE-selectin) levels in serum harvested from middle-aged CD, MSD, CN and MSN animals (CD: n = 19 [11 males; 8 females], MSD: n = 16 [8 males; 8 females], CN: n = 18 [10 males; 8 females], MSN: n = 23 [15 males; 8 females]). **f,** Graph indicates hippocampal IFNγ levels assessed using ELISA in middle-aged CD, MSD, CN and MSN rats (n = 6 males per group). Data are represented as mean ± SEM with individual data points depicted as dots in the graphs (males – lighter shade; females – darker shade). $^{*}p < 0.05$ (Interaction effect on Two-way ANOVA between the variables of MS and NAM); $^{@}p < 0.05$ (compared with CD: Control group on regular drinking water, Tukey's post-hoc test); $^{₹}p < 0.05$ (compared with MSD: MS group on regular drinking water, Tukey's post-hoc test).

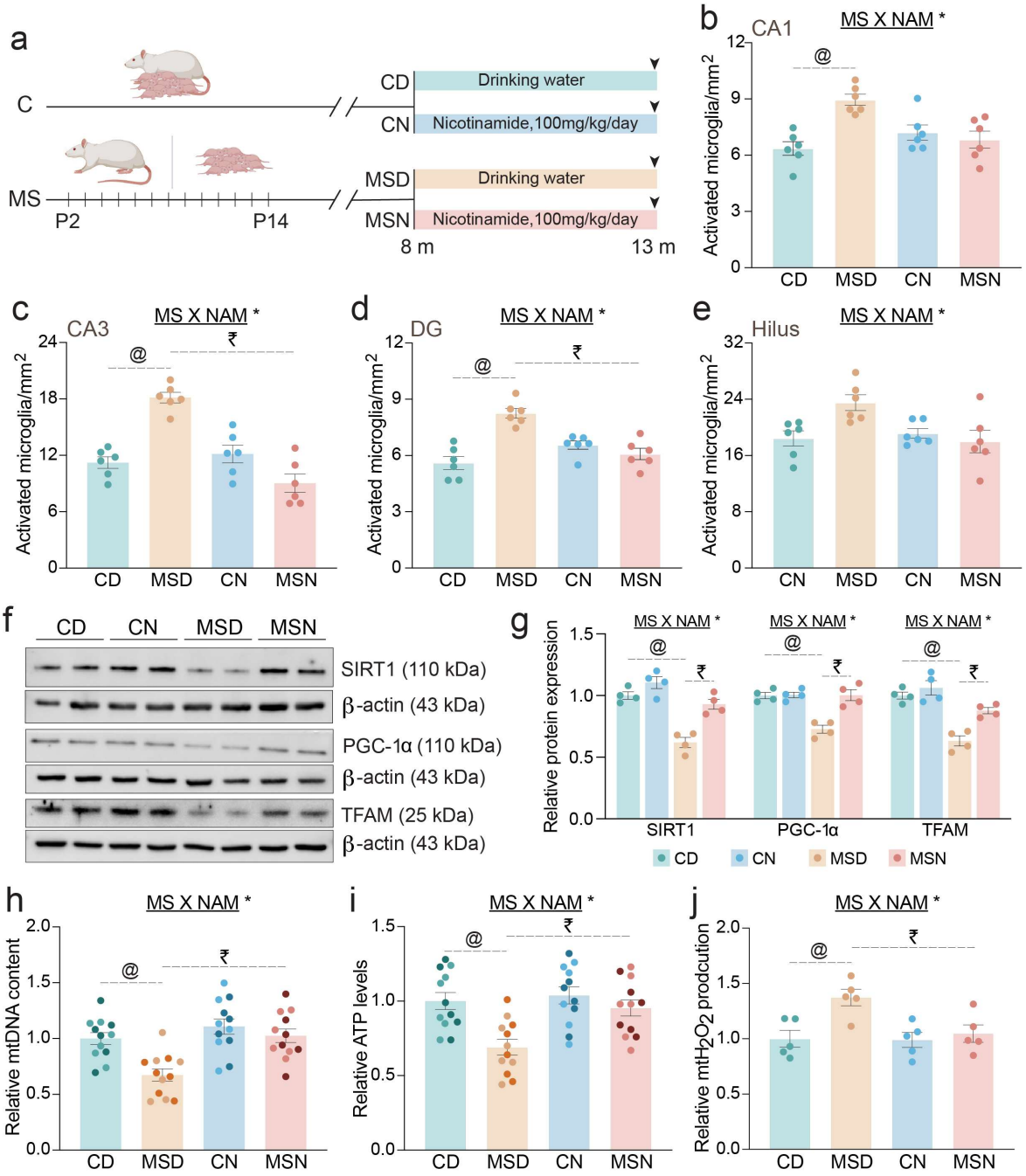

Fig. 7: Nicotinamide supplementation attenuates the neuroinflammation and improves mitochondrial health in hippocampus of middle-aged rats with a history of early-life stress.

a, Shown is a schematic representation of the paradigm for nicotinamide (NAM; 100 mg/kg/day) supplementation through drinking water commencing from 8 months of age for 5 months (CD and MSD: age-matched C and MS animals with regular drinking water; CN and MSN: age-matched C and MS animals with NAM supplemented drinking water) followed by and immunofluorescence studies to assess microglial activation using Iba1. **b-e,** Graphs represent the number of activated microglia/mm^2 in the hippocampal subfields namely (b) CA1, (c) CA3, (d) DG, and (e) Hilus from middle-aged CD, MSD, CN and MSN rats (n = 6

males per group). **f,** Shown are representative western blots for hippocampal protein expression of modulators of mitochondrial biogenesis, namely SIRT1, PGC-1α, and TFAM in the hippocampi of middle-aged CD, CN, MSD and MSN animals, along with β-actin used as a protein loading control. **g,** Graph depicts relative protein expression for PGC-1α, Sirt1, and TFAM in the hippocampi of middle-aged C and MS rats. Data is represented as a fold change of middle-aged C rats (mean ± SEM) with protein expression normalized to β-actin (n= 4 males per group). **h-i,** Graphs represent relative **(h)** mtDNA content and **(i)** cellular ATP levels assessed in hippocampi derived from CD, MSD, CN and MSN animals (n = 12 [6 males and 6 females] per group). **j**, Shown is a graph for mitochondrial reactive oxygen species (mtROS) production in the form of hydrogen peroxide in mitochondria (mtH_2O_2) harvested from hippocampi of middle-aged CD, MSD, CN and MSN rats (n= 5 males per group). Data are represented as mean ± SEM with individual data points depicted as dots in the graphs (males – lighter shade; females – darker shade). $^{*}p < 0.05$ (Interaction effect on Two-way ANOVA between the variables of MS and NAM); $^{@}p < 0.05$ (compared with CD: Control group on regular drinking water, Tukey's post-hoc test); $^{₹}p < 0.05$ (compared with MSD: MS group on regular drinking water, Tukey's post-hoc test).

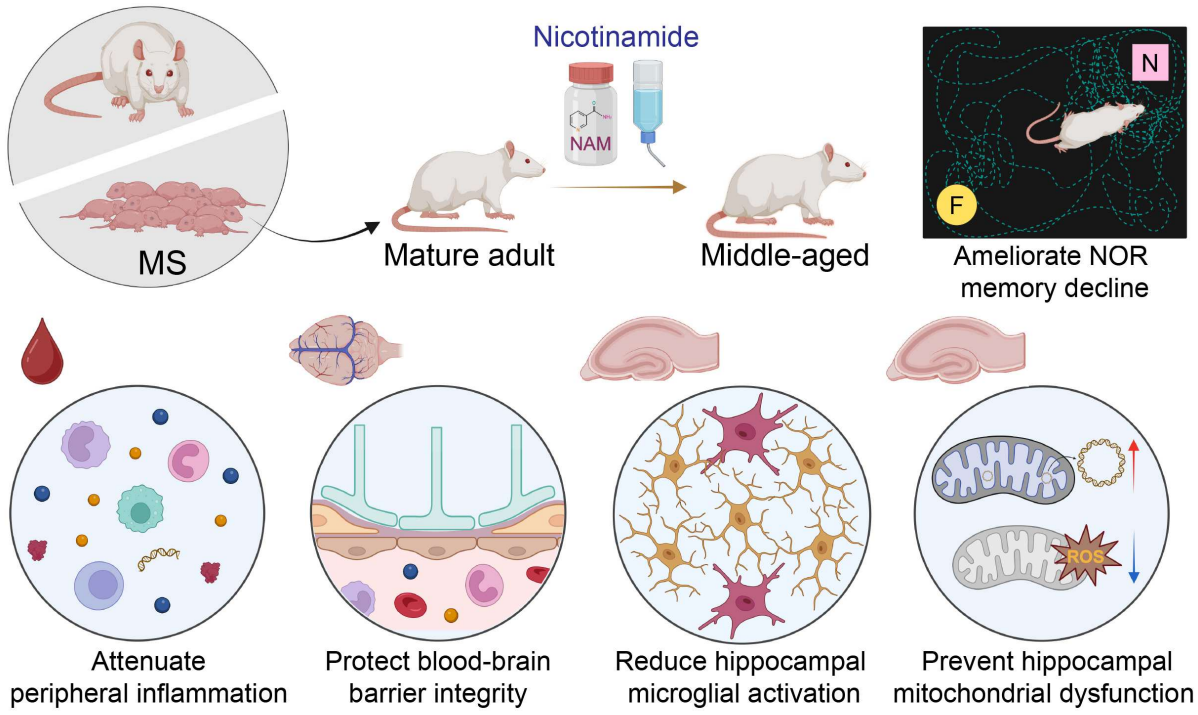

Fig. 8: Nicotinamide supplementation prevents the emergence of early-life stress evoked cognitive decline, peripheral and central inflammation, blood-brain barrier compromise, and hippocampal mitochondrial dysfunction in middle-aged life.
Sprague-Dawley (SD) rats were subjected to early adversity using the MS paradigm, which involved a daily separation (3 hours) of the litters from their dams from postnatal day 2 (P2) to P14. Graphical representation depicts that systemic nicotinamide (NAM; 100 mg/kg/day) supplementation through drinking water commencing from mature adulthood (8 months of

age) for a period of 5 months ameliorates the object recognition memory decline, mitigates peripheral inflammation, preserves BBB integrity, prevent emergence of microglial reactivity in the hippocampi, protect deterioration of mitochondrial health in the hippocampi of middle-aged animals with a history of MS. (Key: F- familiar object, N- novel object).

Supplementary Files

This is a list of supplementary files associated with this preprint. Click to download.

- ExtendeddatalegendsChaudharietal.pdf